PET Agents for Primary Brain Tumor Imaging

Anja G van der Kolk, MD PhD[1,2], Dylan Henssen, MD PhD[1], Harry W Schroeder III, MD PhD[3], Lance T Hall, MD[3]

[1]Department of Medical Imaging, Radboudumc, Nijmegen, the Netherlands; [2]Donders Center for Cognitive Neuroscience, Nijmegen University, Nijmegen, the Netherlands; [3]Department of Radiology and Imaging Sciences, Emory University, Atlanta, GA, USA

Author for correspondence: Anja G van der Kolk, Department of Medical Imaging, Radboudumc, Nijmegen, the Netherlands; Anja.vanderKolk@radboudumc.nl

Cite as: van der Kolk AG, Henssen D, Schroeder HW III, Hall LT. *PET Agents for Primary Brain Tumor Imaging*. Brisbane (AU): Exon Publications; 2023. Online first 20 Nov 2023.
Doi: https://doi.org/10.36255/pet-agents-for-pimary-brain-tumor-imaging

Note to the Reader: This open access monograph (ISBN: 978-0-6458663-0-8) has been peer reviewed and accepted for publication, but not yet copyedited or typeset. This was published under the *Rapid Publication* service. The monograph in its final form will be copyedited and published in pdf, html, and xml formats in December 2023 as shown under *Catalogue*. The citation details will not change even after the publication of the monograph in its final format. The publisher is *Exon Publications*, Brisbane, Australia.

ABSTRACT

The role of molecular imaging with positron emission tomography (PET) for diagnosis, treatment planning and post-treatment monitoring of brain tumors has grown substantially in the last decades. In the last 25 years, almost 50 different PET agents have been developed and tested in human clinical studies. While some of these PET agents are yet to make their way into clinical practice, others have already established pivotal roles in brain tumor imaging. Although all these agents share an affinity for brain tumor cells, they target different tumor-altered molecular pathways within these cells: some agents are taken up by the cell through overexpressed transporters and become trapped, altered, or incorporated into upregulated metabolic pathways, while other agents bind to overexpressed receptors or to cells

present in the tumor microenvironment. In this monograph, we explore the major genetic and molecular changes characteristic of brain tumors, how they are used by PET agents to gain access to tumor cells and their environment, and how this translates to uptake in clinical practice. Gaining insight in these processes is essential for correct image interpretation and helps to understand why some agents are more successful than others.

Keywords: brain tumors; glioma; molecular imaging; PET; uptake mechanisms

Running title: PET agents for primary brain tumor imaging

INTRODUCTION

Primary brain tumors are devastating tumors with high morbidity and mortality, even after optimal treatment consisting of surgery and chemoradiation (1). Imaging and histological assessment of mutation status play indispensable roles in the diagnostic workup, treatment, and follow-up of these tumors. Although MRI (magnetic resonance imaging) is the primary imaging technique for both initial diagnosis and subsequent follow-up, structural sequences often fall short in distinguishing between WHO (World Health Organization) types and grades (2). Image contrast in MRI relies primarily on imaging (protons in) water, which is the most abundant substance in the human body and, consequently, not very specific for any type of tissue in particular. In addition, some advanced imaging techniques such as diffusion and perfusion MRI may lack specificity in tumor assessment. These limitations reduce the value of conventional MRI in primary brain tumor assessment.

Molecular imaging techniques like molecular MRI and positron emission tomography (PET) on the other hand generate image contrast by visualizing or measuring specific *molecular characteristics* of tissues. Since tumors are characterized by various grades of molecular dysregulation that depend on and are often specific for the type of tumor, these imaging techniques could be more tumor-specific than conventional MRI. Indeed, molecular MRI sequences like MR spectroscopy and chemical exchange saturation transfer have shown promise in better delineating brain tumors and differentiating between brain tumor types. However, current limitations in spatial and spectral resolution significantly affect the success rate of metabolic MRI (3). PET has been the classic molecular imaging technique over the last decades, and has a strong track record for cancer imaging in the body. Instead of measuring the *static* presence of molecules like in MR spectroscopy, PET images represent a *dynamic* process of PET agent uptake that

is characteristic of the particular tissue. In addition, PET agents can be designed to target tissue-specific metabolic pathways and molecules. Compared to MRI, these advantages together could result in higher brain tumor specificity by providing a more complete picture of the molecular phenotype of brain tumors.

UNDERSTANDING UPTAKE OF PET AGENTS

Over the last 25 years, more than 50 different PET agents have been evaluated for primary brain tumor imaging in humans. Most agents have been designed to target certain molecules, such as transporters or receptors, that are associated with specific metabolic pathways that are known to be upregulated or even thought to be unique in brain tumor tissue. Notwithstanding their high target specificity, success rates of these agents have varied widely because uptake is a dynamic process that depends on more than just target binding; it also involves crossing the blood-brain barrier (BBB) and becoming retained (or not) in the tumor cell through simple trapping or by metabolic incorporation. These processes depend heavily on the structure of the specific PET agent and which receptor or transporter it targets. An additional complicating factor is the growing insight that current target molecules and associated pathways may be less tumor-specific than previously thought.

Understanding the underlying mechanisms of PET agent transport, binding or uptake, and trapping is important for correct interpretation of PET images in clinical practice, and to aid in choosing the most appropriate agent for the particular tumor type or individual patient case. In this monograph, we explore the major genetic and molecular changes characteristic of brain tumors, how they are used by PET agents to gain access to tumor cells and their environment, and how this translates to uptake in clinical practice. Several in-depth discussions on the value of specific groups of PET agents in clinical diagnosis and follow-up of brain tumors can be found in the literature (4-7); a concise overview of clinical trial results is given in **Table 1**.

GENETIC CHANGES IN BRAIN TUMORS

Brain tumor cells are characterized by increased, uncontrolled proliferation and a tendency to invade healthy tissues, sometimes accompanied by spread to distant sites. These features result from combinations of genetic changes, like mutations and deletions, which vary between different tumor types and often even within the same tumor (8, 9). Many genetic changes have been recognized to play a role in brain tumor development, the most important of which will be briefly described below (**Table 2**).

PI3K-AKT-mTORC signaling pathway

Both increased tumoral secretion of growth factors, for example, PDGF (platelet-derived growth factor), EGF (epidermal growth factor) and TNF-α (tumor necrosis factor-alpha), as well as mutation or deletion of the tumor suppressor gene PTEN (phosphatase and tensin homolog) will stimulate this pathway leading to increased energy metabolism and angiogenesis. Two other genetic alterations that affect this pathway are loss or inhibition of the p53 protein (see below) that normally stimulates expression of PTEN, and mutation of the EGF receptor (EGFR) gene with subsequent increased signaling of EGFR and pathway upregulation (10).

Ras-Raf-MEK-ERK(MAPK) signaling pathway

In addition to the increased growth factor secretion, several genetic alterations also directly affect the MAPK (mitogen-activated protein kinase) pathway and lead to cell cycle progression: NF1 (neurofibromatosis-1) mutations activate Ras independent of growth factors, while BRAF (B-Raf proto-oncogene) mutations exert the same effect on Raf. More indirectly, overexpression of the protein COX2 (cyclooxygenase-2) will lead to increased pathway stimulation through EGFR (11).

MYC protein

The MYC protein functions as a general transcription factor for a variety of genes associated with normal development; overexpression will therefore affect many, if not all, cellular pathways (some are illustrated in **Figure 1**). MYC sustained, or over-expression, can be found in virtually all tumor types, and is seen as a major driving force in oncogenesis (12, 13). In brain tumors, one of its main roles has been regulation and proliferation of a highly malignant tumor cell subtype (tumor stem-like cell) (14).

p53 protein

Mutations of the TP53 tumor suppressor gene (most common) or inactivation of its protein p53 occur in virtually all tumor types (15). p53 normally regulates DNA damage repair (including oncogenic alterations), cell cycle progression and apoptosis (16). Causes of inactivation include deletions or mutations in the INK4/ARF (ADP ribosylation factor) tumor suppressor locus and increased MDM2/4 (E3 ubiquitin-protein ligase-2 and -4) gene expression. MDM2 and MDM4 are proteins that both directly inhibit activity of p53 as well as stimulate its degradation (17). The INK4/ARF locus harbors genes encoding ARF, a protein that normally inhibits MDM2 from impeding p53 function, thereby stabilizing and activating p53 (18).

Rb1 protein

This tumor suppressor protein (retinoblastoma-1) normally inhibits CDKs (cyclin-dependent kinases), stabilizes chromosome structure, and binds E2F transcription factors, thereby inhibiting gene transcription and subsequent cell cycle progression. Its functional impairment may be caused by direct mutation of its gene or (more commonly) increased expression of its regulators (cyclin D, CDK4, CDK6) that cause detachment of E2F from Rb (19). Additionally, Rb function can be influenced by deletions or mutations in the INK4/ARF tumor suppressor locus. Next to ARF, this locus also holds genes for proteins INK4a and INK4b that inhibit activity of CDK4/6 and (indirectly) cyclin D (18).

MGMT protein

Methylation of the MGMT (O^6-methylguanine-DNA-methyltransferase) gene promoter renders gene transcription impossible and leads to decreased amounts of the DNA repair protein MGMT and, consequently, decreased DNA repair. A 'positive' methylation status will enable oncogenic genetic alterations to survive; on the other hand, DNA damage caused by chemotherapeutics will also evade repair, leading to chemotherapy-induced apoptosis. This is illustrated in patients with MGMT promotor methylated tumors who profit more from chemotherapy than those without 'positive' methylation status (20).

IDH protein

The discovery of the IDH (isocitrate dehydrogenase) mutation caused a radical rethinking of brain tumor development and classification (21). Mutations in the IDH1 and IDH2 gene are neomorph, resulting in an IDH protein with a new function: converting α-KG (alpha-ketoglutarate) to 2HG (2-hydroxyglutarate), which subsequently accumulates within the tumor cell and ultimately blocks cellular differentiation. The tumor cell will compensate for the altered flux of α-KG by increasing glutaminolysis. IDH-mutated tumors are often associated with younger age at diagnosis and better prognosis (22).

ATRX & TERT

Mutations in telomere maintenance genes ATRX (alpha-thalassemia / mental retardation syndrome X-linked) and TERT (telomerase reverse transcriptase) are often seen together with IDH mutations. In general, the amount of cell divisions is limited by the length of telomeres, DNA-protein complexes capping chromosome ends, protecting them from end-to-end fusion and apoptosis. Successive cell divisions shorten telomeres, ultimately leading to cellular 'ageing' and death. TERT and ATRX are able to reverse telomere shortening by increasing telomerase activity and alternative lengthening of telomeres,

respectively. Normally, these genes are downregulated; however, in tumor cells, (promotor) mutations will activate TERT and ATRX, resulting in telomere conservation and increased cellular survival (22, 23).

1p19q co-deletion

This genetic alteration has been classified as a key molecular feature of oligodendroglioma in the WHO classification of brain tumors (21). Although its exact role in tumorigenesis has not been elucidated yet, recent histopathological studies have shown an association with immune suppression in the tumor microenvironment (24).

ENERGY METABOLISM IN BRAIN TUMORS

While several of the above described genetic changes individually affect treatment options and can be used for prognostication, they have one main effect: the production of a variety of abnormal proteins and dysregulation of molecular pathways within cells (the tumor's *molecular phenotype*) that ultimately promote cell cycle progression, proliferation and survival (2, 25). The most important dysregulated pathways for PET agent uptake are described below, while a more detailed overview can be found in Figure 1. Readers are also referred to two excellent reviews by DeBerardinis et al. (general cancer metabolism) and Park et al. (focus on gliomas) (26, 27).

Increased energy metabolism

A primary feature of tumor cells is upregulation of their energy metabolic pathways. Cells produce energy primarily by glucose degradation (glycolysis), with either subsequent incorporation of pyruvate in the TCA cycle and oxidative phosphorylation – yielding 36 molecules of adenosine triphosphate (ATP) – or degradation into lactate – yielding only 2 ATP but 10-100 times faster. When necessary, they may also use amino acids like glutamine as well as fatty acids and molecules like acetate as substrates. Multiple genetic changes can cause upregulation of these pathways in tumor cells and are summarized in Table 2 (10, 26, 28). To sustain these pathways, tumor cells will overexpress plasma membrane transporters, allowing increased inflow of energy substrates, or upregulate glutaminolysis and, to a lesser extent, fatty acid and acetate degradation (29). Upregulation of energy metabolic pathways enables tumor cells to proliferate as well as support all other energy-demanding metabolic processes. As a side-effect, their seemingly counterintuitive switch to less energy-efficient aerobic glycolysis (Warburg effect) stimulates angiogenesis and suppresses the innate immune response through production of lactate, which has emerged as a major factor in oncogenesis (30-32). The subsequently increased reactive oxygen

species (ROS) production, which is potentially toxic, can be neutralized by cystine influx through the often overexpressed system x_{CT}^- transporter (33).

Increased fatty acid, protein, amino acid, and nucleotide synthesis

Increased cellular proliferation necessitates large amounts of cellular building blocks, like nucleotides for deoxyribonucleic acid (DNA) replication, fatty acids for plasma membrane construction and amino acids for protein synthesis. Apart from overexpressing transporters for increased inflow of these building blocks, tumor cells will also upregulate the associated metabolic pathways, i.e. protein, amino acid, fatty acid and nucleotide synthesis. The increased energy production discussed before facilitates these processes.

INCREASED ANGIOGENESIS

To sustain increased inflow of nutrients and building blocks, a high enough concentration of these molecules *outside* the cell will be required. Tumor cells facilitate this by initiating and upregulating several pathways of neovascularization, including vascular co-option, vasculogenesis, and (most commonly) angiogenesis, hereby significantly increasing the number of vessels supplying the tumor. Angiogenesis is a complex process in which tissue cells and their surrounding stroma interact and produce growth factors like vascular endothelial growth factor (VEGF) that attract and stimulate endothelial and mesenchymal cells to form new (micro)vessels (16, 34, 35). This will ensure sufficient supplies of nutrients and other molecules to reach the tumor (36). Of note, these tumor microvessels are often leaky and dilated because of continued pro-angiogenic signaling that results, amongst others, in mixing of tumor cells with endothelial cells and an absence of stabilizing pericytes. This not only decreases the supply of nutrients like glucose, but also the oxygen tension. Hence, this poses a clinical dilemma when interpreting uptake on PET images (34, 35).

The tumor microenvironment

Tumor cells establish the tumor microenvironment (TME), a complex network with various non-malignant cells like fibroblasts, endothelial and inflammatory cells, surrounded by extracellular matrix rich in proteins, cytokines and other signaling molecules. Interaction between the TME and tumor cells further facilitates tumor growth and angiogenesis, invasion and migration (metastasis), and plays an important role in suppressing the body's natural immune reaction to tumor cells (37). Many of these interactions rely on increased expression of tumor cell receptors that subsequently cause upregulation of their associated signal transduction pathways. In more malignant brain tumors, they are also facilitated

by hypoxia due to a lack of sufficient vasculature, dysfunctional (leaky) tumor microvessels, or both. Although tissue with very low pO_2 will eventually die and become necrotic, mild to moderate hypoxia can be survived and is used to suppress the immune system and stimulate angiogenesis, tumor cell invasion and migration (38, 39). It also creates a relative resistance to radio- and chemotherapy, e.g. by inducing cell cycle arrest in the phase least sensitive to ionizing radiation, by limiting the detrimental effect of free radicals produced by interaction of radiation with water molecules, or by affecting delivery and uptake of chemotherapeutic drugs (39, 40). Consequently, a 2-3x higher radiation dose is necessary for hypoxic tissue to obtain effects equivalent to normoxic tissue (40). Other pathways of immune system inhibition include VEGF secretion and secretion of kynurenine, both of which attract immunosuppressive regulatory T cells (41) that inhibit the anti-tumor immune response and stimulate angiogenesis through suppression of helper T cells (35). The processes of immune suppression and invasion / migration involve many more mechanisms; however, only those with a role in PET agent uptake have been discussed here (42).

Targeting tumor molecular pathways for PET imaging

Most PET agents for brain tumor imaging have been designed to use the dysregulated pathways by targeting either upregulated transporters or -receptors on the tumor cell surface. They can be categorized based on the specific pathway they target: (i) increased energy metabolism and building block synthesis (glucose, amino acids and other nutrients); (ii) sustained cell cycle progression; (iii) increased angiogenesis; and (iv) the tumor microenvironment (hypoxia, growth factors). The following paragraphs discuss all PET agents used for this purpose in the last 2½ decades under nine broad categories. First, the monograph focuses on PET agents that target energy metabolism and building block synthesis under four sections: glucose-based agents, natural and non-natural amino acid-based agents, other nutrient-based agents, and agents not based on glucose or other nutrients. This is followed by five sections on various PET agents that target various aspects of tumor biology such as cell cycle progression, angiogenesis, tumor microenvironment, multiple pathways, with the last section on pet agents ‘incidentally’ found to accumulate in brain tumors. An overview of expression patterns of the targeted transporters and receptors can be found in **Table 3**.

GLUCOSE-BASED AGENTS

Glucose uses both the facilitated diffusion glucose transporter (GLUT) family and the sodium-glucose linked transporter (SGLT) family to enter brain cells. Due to increased glycolysis and the TCA cycle, these transporters are upregulated in brain tumor cells, resulting in high concentrations of glucose inside

the cell that facilitate energy production (10, 43). ^{18}F-FDG and ^{18}F-Me-4DFG are two glucose analogues that use the increased number of glucose transporters to image brain tumor cells. ^{18}F-FDG mainly uses GLUT-1 and to a lesser extent GLUT-3, both which are present on the BBB (Table 2); after entering the cell, it is phosphorylated and becomes trapped as ^{18}FDG-6-phosphate (**Figure 2**). ^{18}F-Me-4FDG uses SGLT2, which is *not* present on the healthy BBB, rather only on endothelial cells of tumor vasculature (Table 3); after entering the cell it becomes trapped without phosphorylation (Figure 2). In clinical practice, uptake of either agent will reflect overexpression of the transporters and therefore (indirectly) increased energy metabolism. The BBB does not hamper the uptake of ^{18}F-FDG, and the uptake of ^{18}F-Me-4FDG will additionally reflect increased tumor vasculature +/- BBB leakage. Since energy metabolism generally increases with increasing malignancy grade, ^{18}F-FDG has often been used to differentiate between WHO grades, and recently even between IDH-mutated and IDH-wildtype tumors (44). It can also help differentiate tumor recurrence from treatment-related changes, and recent radiomics techniques with also show promise in predicting Ki-67 expression and patient prognosis non-invasively (45, 46). The main limitation of ^{18}F-FDG lies in the generically high rate of glucose metabolism in the healthy cerebral cortex, leading to low tumor-to-normal-tissue (T/N) ratios for most tumors except those with very high cellular density and metabolic rate, like lymphoma (47). ^{18}F-Me-4FDG does not have this problem since it does not cross the healthy BBB, causing a very low uptake in healthy brain tissue and consequently high T/N ratio, which is its main advantage over ^{18}F-FDG (**Figure 3**) (48). For both agents, a major limitation is their intrinsic low tumor specificity: increased glucose consumption is also seen in other non-oncological processes such as (acute) inflammatory tissue, although ^{18}F-Me-4FDG might prove more tumor-specific due to its inability to cross the BBB (49).

NATURAL AND NON-NATURAL AMINO ACID-BASED AGENTS

Amino acids enter cells through a variety of transporters, the most important of which are system L (LAT) and system ASCT (alanine/serine/cysteine-preferring transporters) (50). LAT1 and ASCT2 in particular have been found overexpressed in brain tumor cells and are therefore the main targets for PET agents (Figure 2) (51). In the brain, LAT1 is mainly expressed by tumor cells and endothelial cells, facilitating easy BBB crossing of PET agents that use this transporter, while LAT2 is also expressed in non-tumor cells, and ASCT is minimally expressed in normal brain. On the other hand, ASCT1 and -2 are not expressed on endothelial cells and therefore do not facilitate transport across the BBB (50, 52). Both types of transporters can also be found in other pathological tissues like (chronic) inflammatory B- and T cells. After entering the cell, PET agent assimilation depends on whether the amino acid's molecular structure has been significantly altered (Figure 2). Although all amino acid based agents,

especially those using LAT1-2, have some background uptake because they can be used for energy production and protein synthesis in healthy brain parenchyma, or become part of healthy cellular amino acid pools, this is significantly less than ^{18}F-FDG (50, 53).

LAT-dependent agents

Of the eight amino acid-based agents using LAT transporters, ^{11}C-MET, ^{11}C-TYR, ^{18}F-FDOPA, ^{18}F-FAMT and ^{18}F-FIMP are currently believed to solely use LAT1, which is mainly expressed on tumor- and endothelial cells and will therefore easily cross the BBB. After entering the tumor cell, only ^{11}C-MET and ^{11}C-TYR become incorporated into proteins, and to a lesser extent into phospholipids and DNA, especially ^{11}C-MET (Figure 2) (54, 55). In clinical practice, uptake of these two agents will reflect overexpression of LAT1 as well as (for ^{11}C-MET partial) increased protein synthesis indicative of increased metabolism. One must keep in mind that uptake of PET agents such as ^{11}C-MET may also potentially reflect a contribution from a more nonspecific process such as blood-brain barrier disruption that can occur with benign brain pathologies such as vascular lesions, posttreatment changes, tumefactive multiple sclerosis, and infection (56). ^{18}F-FDOPA and ^{18}F-FAMT do not become incorporated into proteins but instead stay inside the cytoplasmic amino acid pool (Figure 2); uptake in practice will therefore reflect LAT1 overexpression similar to ^{11}C-MET and ^{11}C-TYR but with only indirect evidence for increased protein synthesis (57-59). An additional disadvantage of ^{18}F-FDOPA is its incorporation into dopaminergic neuron metabolism, causing high uptake in the basal ganglia that can significantly limit tumor assessment (60). However, ^{18}F-FDOPA reportedly shows greater contrast for lesions outside the striatum when compared to ^{18}F-FET (61). Of note, there is evidence suggesting that LAT1 expression alone does not entirely explain intensity variation in uptake of ^{18}F-FDPOA in brain tumors (57).

Moreover, like ^{11}C-MET discussed above, ^{18}F-FDOPA is another example of a PET agent that has been shown to localize to pseudotumoral brain lesions possibly due to blood-brain barrier permeability, macrophage response, and/or adjacent reactive astrogliosis (61, 62). ^{18}F-FIMP is a new agent that shows higher accumulation in higher-grade gliomas compared to lower grades and non-gliomas in a small first-in-human study, and might be better retained in the cytoplasm than e.g., ^{18}F-FET below (63). The limited data so far, however, are unclear regarding its assimilation: it is not incorporated into proteins but whether it solely becomes trapped in the cytoplasm or is partially metabolized is as yet unknown (64). Uptake in clinical practice is therefore so far similarly interpreted as for ^{18}F-FDOPA and ^{18}F-FAMT. ^{11}C-MCYS and ^{18}F-FET use either LAT1 or LAT2 which is also expressed in non-tumor cells; after entering the tumor cell, they stay inside the cytoplasmic pool (Figure 2). It is assumed that ^{18}F-FET transport is

mediated predominantly by use of the LAT1 transporter, since LAT2 transporters are not expressed on the luminal side of the BBB (65). The use of LAT2 may account for the disappointing results of ^{11}C-MCYS in a recent animal study, showing significantly higher healthy brain parenchymal uptake than ^{11}C-MET, even though preliminary human results were promising (54, 66, 67). In clinical practice, uptake can be interpreted similar to ^{18}F-FDOPA and ^{18}F-FAMT with the addition of LAT2 overexpression. Interestingly, ^{18}F-FET is one of the only amino acid-based agents for which time-activity curves, reflective of dynamic uptake, provide additional information on tumor grading and prognosis (68, 69). This suggests that the uptake mechanism may be slightly different from the other agents and although the main route of uptake uses the LAT1 transporter, studies also point to uptake using the Na^+-dependent amino acid transporter $B^{0,+}$ and $b^{0,+}$. This uptake mechanism is dependent on the specific cell type and the differences between intracellular and extracellular amino acid concentrations (70). ^{18}F-OMFD is a metabolite of ^{18}F-FDOPA with very limited and dated information on uptake and clinical value and will therefore not be discussed.

Even more advanced kinetic analysis will be necessary to interpret uptake of ^{11}C-AMT. This agent, similar to its associated amino acid tryptophan, enters cells through LAT1 and is not only used for protein synthesis but can also be incorporated into the kynurenine pathway (71). In tumors, upregulation of this pathway by increased activity of one or both of its two main enzymes, indoleamine 2,3-dioxygenase (IDO) and tryptophan 2,3-dioxygenase (TDO), plays a key role in escaping the body's immune response to the tumor (Figure 1 and Figure 2). Although IDO overexpression is mainly a characteristic of low-grade astrocytic tumors, uptake of ^{11}C-AMT can be seen in both low- and high-grade tumors. This suggests that the factors influencing uptake in low- and high-grade brain tumors might be different, with increased IDO activity dominating uptake in low-grade tumors, while increased transport of ^{11}C-AMT into tumor cells might dominate in high-grade tumors. In clinical practice, uptake will reflect either an upregulated kynurenine pathway associated with immunosuppression, or increased transport due to LAT1 overexpression / increased vasculature, depending on the tumor type. High uptake in contrast-enhancing tumor regions is strongly prognostic for overall survival (72). A drawback is its extensive use for protein synthesis in healthy brain parenchymal cells, decreasing T/N ratios to levels quite similar to ^{18}F-FDG (73, 74). The outlier ^{18}F-FBPA is not an amino acid but selectively uses LAT1 to gain access to the tumor cell (Figure 2). It was primarily created to assess efficacy of boron neutron capture therapy with boronophenylalanine (BPA) in various tumor types, including gliomas (75, 76). It may be more tumor-specific than agents that also rely on LAT2 for access to cells (77). Nevertheless, subsequent studies have questioned whether FBPA can accurately estimate BPA distribution considering its distinct

molecular structure, and it is relatively unstable with fast deboronation. ^{18}F-FBY (fluoroboronotyrosine) has recently been introduced as a more stable alternative; it is a boron-derived tyrosine using the same LAT1 transporter, and while it is amino acid-based (tyrosine) it will not be recognized as such by the cell due to its aberrant structure and will therefore be quickly excreted instead of becoming either trapped in the cytoplasm or incorporated (Figure 2), which leads to a lower background activity than other amino acid-based agents. In addition, like other agents using the LAT1 transporter, uptake will not depend on BBB permeability; indeed, ^{18}F-FBY uptake has been seen in non-enhancing brain tumor areas and shows a pattern distinct from the pattern of enhancement. Uptake will therefore primarily reflect overexpression of the LAT1 transporter. An additional advantage is that FBY can be used for treatment by substituting ^{18}F for ^{19}F for boron neutron capture therapy; however, treatment results with this agent have not yet been published (78, 79).

ASCT-dependent agents

Only three agents – ^{18}F-FGln, ^{11}C-ACBC and ^{18}F-FACBC – use ASCT(2) transporters. Although ASCTs are absent on endothelial cells, all three agents have shown to readily cross the BBB, probably through LAT transporters. Their main advantage over LAT-associated agents stems from the fact that ASCTs are minimally expressed in normal brain, leading to very low uptake in healthy tissues (**Figure 4**) (80). After entering the tumor cell, only ^{18}F-FGln becomes incorporated into proteins; ^{11}C-ACBC and ^{18}F-FACBC (also called ^{18}F-Flucoclovine), two non-natural amino acid-based agents, cannot be used in metabolic pathways and will instead be trapped in the cell (Figure 2) (29). In clinical practice, uptake of all three agents will reflect overexpression of ASCT2 (and LAT for crossing the BBB); direct evidence for increased protein synthesis however is only seen for ^{18}F-FGln uptake (49, 52, 81, 82).

Non-LAT, non-ASCT PET agents

Three amino acid-based agents use transporters other than LATs or ASCTs. ^{18}F-FSPG crosses the plasma membrane through system x_{CT}^- (Figure 2), a glutamate/cystine exchanger which is absent from the BBB and becomes overexpressed in response to increased levels of ROS, a byproduct of tumor-upregulated metabolic pathways (Figure 1). Although background uptake is very low, in clinical practice uptake will reflect at least increased BBB permeability, with or without increased oxidative stress / ROS production and indirectly increased metabolic activity (83). Tumor cell specificity however may be higher than other amino acid-based agents because system x_{CT}^- is not expressed on inflammatory cells (49). There are also significant differences in the uptake curves of primary brain tumors, though not metastases, of lesions with good versus poor outcomes (84). D-cis-^{18}F-FPro is transported across the plasma membrane via the

proline transporter PROT. Uptake is thought to represent pathological cell death / necrosis (Figure 2), as opposed to the apoptosis-targeting PET agent ^{18}F-ML-10 (see paragraph 'PET agents targeting multiple pathways'). However, conflicting results regarding its transport through the BBB currently restrict any certain statements regarding its uptake in clinical practice (85). ^{11}C-MeAIB uses the system A neutral amino acid transporter to gain access to the tumor cell, after which it becomes trapped (Figure 2) (86). In addition to the natural amino acids alanine, serine and cysteine, the system A transporter accepts MeAIB (an artificial amino acid) as a unique substrate, and it becomes overexpressed with increasing proliferation rate and malignant transformation in several carcinoma cell lines (87, 88). While considered ubiquitously present on mammalian cells, not much is known about the location of system A transporters in the brain except that it is present on the abluminal membrane of the bovine BBB, which explains the poor penetration of ^{11}C-MeAIB through the BBB. In a sole clinical study, ^{11}C-MeAIB could differentiate between low-grade and high-grade astrocytoma with higher T/N ratios than ^{11}C-MET; however, no other studies have been performed since, perhaps because uptake will likely be highly dependent on BBB permeability (86).

OTHER NUTRIENT-BASED AGENTS

Like choline, ^{11}C-choline and ^{18}F-FCho enter brain cells mainly through high-affinity choline transporter 1 (CHT1) and choline transporter-like proteins 1 and 3 (CTL1/3), are subsequently phosphorylated to phosphocholine by choline kinase alpha (CKα) and become incorporated into fatty acids, facilitating cell membrane synthesis (Figure 1 and Figure 2). Increased cellular uptake in brain tumors is caused by both increased expression of CTL1 and increased activity of CKα, facilitating the growing demand for membrane building blocks and energy (89, 90). CTL1 is present on the BBB (Table 3) so uptake will not depend on BBB permeability. In addition, healthy brain cells are generally in a non-dividing state, requiring little choline and thereby causing a very low background uptake (91). Nonetheless, vascularity does seem to play a role in uptake since BBB-lacking tissues as well as benign highly vascularized tumors (e.g., meningiomas) show highest uptake even though their cellular proliferation rates are generally low (92, 93). This might also explain the increased uptake seen in abscesses and other inflammatory processes, further lowering tumor specificity (94). However, there is potential clinical benefit in metabolic post-operative assessment for residual tumor and treatment response assessment in diffuse non-enhancing gliomas where quantitative MRI is limited (95, 96). In clinical practice, uptake will reflect overexpression of CTL1 and/or increased CKα activity and fatty acid synthesis, while vascularity needs to be taken into account.

^{11}C-acetate crosses the plasma membrane through either sodium monocarboxylate cotransporter (SMCT) or monocarboxylate transporter (MCT), the latter of which is present on the BBB (Figure 2 and Table 3). After entering the cell, it becomes primarily incorporated into fatty acid synthesis and the TCA cycle. Increased lactate can further increase uptake of ^{11}C-acetate by hetero-exchange through the MCT transporters; consequently, uptake in patients has been most pronounced in fast-growing, high-grade tumors, although reports vary whether the agent can differentiate between tumor grades (97, 98). In clinical practice, uptake will reflect upregulation of both transporters, fatty acid synthesis and (especially) energy metabolism (99, 100). Drawbacks are the use of (^{11}C-)acetate by healthy brain cells, causing significant background uptake, and uptake in non-tumor tissue like necrotic/fibrotic and granulomatous tissue due to unknown mechanisms (98).

^{13}N-ammonia freely diffuses across the plasma membrane, and once inside the cell becomes converted with glutamate into glutamine by the enzyme glutamine synthetase (GS; Figure 1 and Figure 2) which can subsequently be used for amino acid synthesis. Although GS has been shown to be overexpressed in glioblastomas, it is also abundantly present in normal and reactive astrocytes, causing high uptake in healthy brain tissue, especially cerebral cortex. In addition, the agent does not easily cross the BBB. In clinical practice, uptake will reflect at least increased BBB permeability, with or without increased expression of GS and amino acid synthesis (101).

AGENTS NOT BASED ON GLUCOSE OR OTHER NUTRIENTS

One relatively new agent is not based on glucose, amino acids, or other nutrients, but does target an associated pathway. ^{18}F-DASA-23 binds to pyruvate kinase M2 (PKM2), an isoform of the enzyme pyruvate kinase which catalyzes the last step in glycolysis by converting phosphoenolpyruvate to pyruvate (Figure 1). Contrary to the M1 isoform, PKM2 can be dynamically controlled in its activity, a feature that tumor cells use – via oncogenes c-Myc and HIF-1 – to regulate their need for either anabolic or catabolic metabolism. PKM2 is found ubiquitously in human cells except in muscle, liver and brain, and is preferentially expressed in all types of cancers; in brain tumors, PKM2 expression is mildly increased in grade I to II gliomas but highly expressed in glioblastomas (102). The agent can readily cross the BBB and binding to PKM2 is slowly reversible; however, it is unclear how it is taken up inside the cell, either through a transporter or via passive diffusion (Figure 2). In clinical practice, uptake will therefore reflect PKM2 expression and therefore glycolytic status within tumor tissue *alone*, with a potential but as yet unknown role of the transport mechanism across the cell membrane. This agent could be of lar interest considering the therapeutic efforts of targeting PKM2 for various diseases including

cancer over the last couple of years (103). A first clinical study showed significant binding of ^{18}F-DASA-23 in brain tumors with a high T/N ratio, and a follow-up clinical study is underway (Table 1) (104).

PET AGENTS TARGETING CELL CYCLE PROGRESSION

All four nucleoside-based agents – ^{18}F-FLT, ^{11}C-4DST, ^{18}F-FMAU and ^{11}C-TdR – are based on thymidine, which pairs with adenine in the DNA double helix and is therefore directly involved in cellular proliferation. These agents use equilibrative nucleoside transporter 1 (ENT1) to enter cells (**Figure 5**). Although ENT1 is present throughout the brain including endothelial cells (Table 3), none of these agents can readily cross the BBB leading to a high T/N ratio. In clinical practice, uptake of either agent will therefore reflect at least increased BBB permeability next to ENT1 overexpression (105). After entering the cell, most become phosphorylated by thymidine kinase 1 (TK1), which is cell-cycle dependent and therefore upregulated in tumor cells, or TK2, which is restricted to mitochondria and is cell-cycle independent. Only ^{18}F-FLT and ^{11}C-4DST interact with TK1: ^{18}F-FLT subsequently becomes trapped in the cytoplasm because it lacks an essential hydroxyl group, causing uptake to indirectly reflect increased cellular proliferation, while ^{11}C-4DST becomes incorporated into DNA, thereby *directly* reflecting increased DNA synthesis and proliferation (Figure 5) (105). Kinetic analyses will be necessary to distinguish uptake due to disrupted BBB from that due to increased cellular proliferation(106), decreasing their sensitivity for brain tumor cells compared to amino acid agents like ^{11}C-MET and ^{18}F-FET (**Figure 6**), and they should not be used for e.g., recurrent non-enhancing brain tumors (107, 108). However, uptake of ^{18}F-FLT has been shown to differentiate between grade III and IV gliomas, and is sometimes seen in non-enhancing areas on MRI, suggesting not all uptake is BBB-related; it has also been suggested that even a small number of glioma cells can cause BBB disruption without additional contrast agent leakage (108, 109). Tumor uptake of ^{18}F-FLT can also be used to predict tumor progression in meningiomas (110). Background uptake of ^{11}C-4DST is paradoxically high compared with ^{18}F-FLT, and it has not been studied much (111). ^{18}F-FMAU becomes phosphorylated by TK2, raising the question whether uptake really reflects cellular progression, while ^{11}C-TdR is not used anymore because of its high catabolism into ^{11}C-CO_2 which causes significant background uptake.

PET AGENTS TARGETING ANGIOGENESIS

^{68}Ga-PSMA, ^{18}F-DCFPyL and ^{89}Zr-Df-IAB2M specifically bind to the prostate-specific membrane antigen (PSMA), a receptor thought to induce VEGF-independent angiogenesis in pathological conditions like tumors (**Figure 7**). PSMA is variably expressed on tumoral blood vessels and tumor cells depending on the tumor type, while no expression is seen on healthy brain parenchymal cells or normal

vessels (Table 3); BBB transport will therefore depend on the tumor type (112). Preliminary studies showed high T/N ratios due to the virtually non-existent uptake in the healthy brain. Since all tested tumors showed contrast enhancement, this also raises the question whether uptake on PET images is not simply representative of increased BBB permeability without any role of PSMA. This hypothesis is strengthened by early reports on high uptake in enhancing radiation necrosis and ischemia (113, 114), although more recent studies have demonstrated the ability to distinguish recurrent high-grade gliomas from radiation necrosis (115). In clinical practice, with the limited data so far, uptake will likely reflect BBB permeability, overexpression of PSMA on endothelium or tumor cell (depending on tumor grade), or a combination of both. ^{68}Ga-PSMA is used most often because of its extensive use in prostate cancer, while ^{18}F-DCFPyL is similar but uses ^{18}F as radionuclide. ^{89}Zr-Df-IAB2M is a small part of the PSMA antibody and shows faster clearance, thereby achieving higher T/N ratios than the other two agents (116).

The arginine-glycine-aspartic acid (RGD)-based PET agents ^{18}F-galacto-RGD, ^{18}F-FPPRGD2, ^{18}F-RGD and ^{68}Ga-PRGD2 bind to the receptor integrin $\alpha_v\beta_3$, which is not expressed on healthy brain parenchymal cells but specifically on tumor endothelial cells and, to a slightly lesser extent, on tumor cells themselves (Table 3). In glioblastomas, it promotes tumor cell migration and invasion, angiogenesis, and multiple signaling pathways like the PI3K-AKT pathway leading to cell proliferation (Figure 7). It has also been observed on activated macrophages, suggesting a role within the tumor microenvironment (117, 118). Given the limited clinical data thus far, uptake in clinical practice can reflect overexpression of $\alpha_v\beta_3$ on endothelial cells related to angiogenesis, and/or BBB permeability with overexpression of $\alpha_v\beta_3$ on tumor cells related to a pathway such as angiogenesis, and/or presence of activated macrophages within the tumor microenvironment (119). Future studies, if feasible, will be necessary to elucidate their clinical implications.

PET AGENTS TARGETING THE TUMOR MICROENVIRONMENT

Hypoxia is one of the hallmarks of more malignant, treatment-resistant tumor tissue. Five PET agents (^{18}F-EF5, $^{62}Cu^{2+}$-ATSM, ^{18}F-FAZA, ^{18}F-FRP170 and ^{18}F-FMISO) use this feature to become trapped inside the tumor cell. These agents passively diffuse across the plasma membrane and become reduced to radical anions, a process which is reversible in normoxia and permanent in hypoxia. This leads to macromolecular binding and cellular trapping (**Figure 8**) (120, 121). ^{18}F-FMISO, ^{18}F-EF5 and $^{62}Cu^{2+}$-ATSM are relatively lipophilic and consequently have no difficulty crossing the BBB and plasma membranes, but do so relatively slowly. In the case of ^{18}F-EF5, this leads to prolonged high background uptake which significantly restricts its use, while for ^{18}F-FMISO several hours between injection and

PET imaging are necessary for optimal T/N ratios. $^{62}Cu^{2+}$-ATSM is similarly lipophilic, but instead of binding to macromolecules it undergoes further dissociation into H_2-ATSM and free Cu^{+}, the latter of which can be used by the tumor cell in angiogenesis and protein synthesis (Figure 8) (120). Conflicting results from preclinical and clinical studies regarding the relation between uptake and cellular hypoxia markers, however, have so far limited its use (122). ^{18}F-FAZA and ^{18}F-FRP170 are more hydrophilic and therefore have more difficulty crossing plasma membranes; however, when successful they do so relatively fast. Their advantage is the faster clearance rates resulting in little to no uptake in healthy tissue. In the case of ^{18}F-FAZA, this comes at the cost of an unclear role of BBB permeability; nevertheless, retention of this agent will solely depend on the hypoxic condition in the tumor tissue (121).

^{18}F-FMISO and ^{18}F-FAZA have been most successful; uptake of these agents (either dynamic or static ratios) has been correlated with immunohistochemical hypoxia markers (123). However, due to their different uptake mechanisms, clinical use and image interpretation differ substantially. For ^{18}F-FMISO, uptake in clinical practice is thought to solely reflect decreased pO_2 or hypoxia, and is therefore almost exclusively seen in more malignant tumors (124). Considering its slow clearance from the blood, timing of acquisition after injection is still an area of much debate – varying between 90 minutes and 4 hours in literature – as is the choice between static and dynamic imaging, the latter providing more quantitative measurements (40, 125, 126). Interestingly, while ^{18}F-FMISO is considered to only accumulate in severely hypoxic tissue, uptake partially overlaps with areas of increased metabolism, suggesting that at least parts of these hypoxic areas are still viable (38, 127, 128). For ^{18}F-FAZA, uptake in clinical practice will likely reflect hypoxia, with an additional role of BBB permeability, the extent of which is still not clear. It has a superior blood clearance compared with ^{18}F-FMISO and therefore a higher image contrast. Several preclinical studies have suggested that redox-disbalancing metabolic changes other than hypoxia might play a role in FAZA retention, such as fatty acid metabolism and oncogene expression (129).

PET AGENTS TARGETING MULTIPLE PATHWAYS

Unlike transporters, receptors are often connected to a variety of different intracellular pathways. Hence, most PET agents targeting receptors will therefore indirectly target multiple pathways, like the ones discussed below.

Somatostatin-based (receptor-targeting) agents

Somatostatin binds to one of 5 different somatostatin receptors (SSTRs), of which SSTR1 and -2 are most abundant in the brain (Table 3) (130). In tumors, SSTR activation exerts an anti-tumor effect,

interfering with PI3K- and MAPK pathways and VEGF (Figure 1), and inhibiting cell cycle progression; therefore, overexpression can be seen in low-grade tumors like meningiomas and oligodendrogliomas (130, 131). ^{68}Ga-DOTATATE, ^{68}Ga-DOTATOC and ^{68}Ga-DOTANOC are based on the somatostatin analog octreotide and mainly target SSTR2, especially ^{68}Ga-DOTATATE (Figure 7). None of these agents can cross the intact BBB; uptake in clinical practice will therefore reflect at BBB permeability +/- overexpression of SSTR2, and increased uptake in meningiomas has been associated with faster growth although no correlation was found with tumor grade (132-134). Among brain tumors, ^{68}Ga-DOTA-SSTR is by far the most commonly used PET agent in the evaluation of meningiomas, and pituitary adenomas are the second most common indication (135). Tumor specificity is somewhat limited due to the abundance of SSTRs in the pituitary gland and (variably) on inflammatory (T and B) cells and macrophages (136).

Growth factor-based (receptor-targeting) agents

^{68}Ga-BBN and ^{11}C-PD153035 target growth factor receptors. ^{68}Ga-BBN binds to the gastrin releasing peptide receptor (GRPR), which is involved in PI3K- and MAPK pathways (amongst others) that ultimately lead to glycolysis, fatty acid synthesis and cell progression (Figure 1 and Figure 7). Both low- and high-grade gliomas overexpress GRPR (Table 3) and have shown high uptake of ^{68}Ga-BBN irrespective of grade; however, healthy brain parenchyma shows very low uptake even though neurons express GRPR (Table 3). This suggests that the agent does not cross the BBB even though non-enhancing low-grade tumors do show uptake (137). In clinical practice, uptake might therefore reflect increased cellular metabolism and progression, however with an unclear role of the BBB. Interestingly, Li et al. modified ^{68}Ga-BBN to include a near-infrared fluorescent dye creating a dual-modality imaging probe known as ^{68}Ga-IRDye800CW-BBN that allowed for both preoperative imaging with PET and fluorescent-guided surgery resulting in improved intraoperative glioblastoma visualization and optimal resection (138). ^{11}C-PD153035 binds to the epidermal growth factor receptor (EGFR), which is involved in pathways similar to GRPR, contributes to tumor cell progression and invasiveness (Figure 7), and is overexpressed in a majority of primary glioblastomas. ^{11}C-PD153035 was able to cross the BBB and showed high uptake in EGFR-overexpressing tumors, but its popularity was short-lived, perhaps because therapeutic targeting of EGFR has been disappointing (139).

Adenosine-based (receptor-targeting) agents

^{18}F-CPFPX and ^{18}F-FLUDA both target adenosine receptors. Adenosine and its receptors have multiple roles in the brain, including activation of microglia/macrophages and neurons, regulation of the immune

response, and modulation of neurotransmitter release and neuronal plasticity. In brain tumors, increased levels of adenosine – created by the tumor microenvironment, e.g., hypoxia – are thought to inhibit T cells leading to immune response evasion; the effect of adenosine on tumor cell proliferation (through the MAPK signaling pathway) has been more controversial, with equal reports on anti-tumor effects (140). ^{18}F-CPFPX is a specific ligand for the adenosine receptor A_1AR (Figure 7) and in one preliminary study showed uptake restricted to the peritumoral tissue, suggesting a possible cellular reaction of this tissue to infiltrating tumor cells; however, T/N ratios were low and the at that time ambivalent role of adenosine receptors likely precluded further investigations (141). ^{18}F-FLUDA was introduced more recently and is a specific ligand for the adenosine receptor A_{2A}AR which has the highest expression in the striatum where it interacts with dopamine signaling (142). More than A_1AR this receptor plays a crucial role in inflammatory processes involving microglia. ^{18}F-FLUDA also specifically links with B-lymphocytes and a recent first-in-human study demonstrated the potential to distinguish primary central nervous system lymphomas from glioblastoma (143). Nevertheless, whether these agents readily cross the BBB is as yet unknown, precluding clear statements on uptake interpretation.

Translocator protein (TSPO) agents

^{11}C-PK11195 and ^{18}F-DPA-714 selectively bind to the mitochondrial translocator protein (TSPO) located on the outer mitochondrial membrane (Figure 7). In the brain, TSPO helps maintaining homeostasis and is thought to be involved in steroidogenesis through intramitochondrial cholesterol metabolism (producing ROS as a byproduct). Although its role in oncogenesis has yet to be elucidated, it has been found overexpressed in neurological diseases associated with neuroinflammation – being upregulated in pro-inflammatory microglia/macrophages and astrocytes in preclinical studies – and its presence is increased in glioblastomas tumor microenvironment (144-146). In gliomas, overexpression is associated with a higher malignancy grade, increased invasiveness and a poor survival. Interestingly, due to the high expression of TSPO on inflammatory cells including those recruited by the tumor (like glioma-associated microglia/macrophages), TSPO-targeting agents might be able to directly visualize the tumor microenvironment (Table 3) (147). Both agents can passively diffuse across the BBB so uptake will not depend on BBB permeability, but how they subsequently reach the cell nucleus is less clear, limiting clear statements on uptake interpretation (147-149).

While not targeting the mitochondrial membrane, ^{18}F-FDHT does target a receptor *inside* the tumor cell, namely androgen receptor (AR), a nuclear membrane receptor that is translocated into the nucleus after binding with 5α-dihydrotestosterone (derivative from testosterone in males and dehydroepiandrosterone

in females). Within the nucleus, it functions as nuclear transcription factor, facilitating transcription of genes promoting cellular growth and survival. AR has been found overexpressed in glioblastoma nuclei and surrounding tumor-associated arteries. Although the exact role of AR in brain tumorigenesis has not been elucidated yet, AR antagonists have been shown to suppress MYC expression, suggesting a role in tumor cell maintenance and proliferation (Figure 7) (150, 151). A preliminary study showed uptake in glioma and a very low target-to-background ratio; however, whether the agent crosses the BBB and how it enters tumor cells is unknown, limiting clear statements on uptake mechanisms and its clinical interpretation (Table 1) (152).

Transporter-targeting agents

Three targeted *transporters* also indirectly target multiple pathways. For entering tumor cells ^{124}I-CLR1404 uses lipid rafts, dynamic domains within the plasma membrane that are overexpressed on tumor cells and support a variety of signaling pathways. ^{124}I-CLR1404 is thought to cross the BBB through passive diffusion – although there have been some contradictory results – and becomes trapped once inside the tumor cell. In clinical practice, uptake will reflect lipid raft overexpression and indirectly upregulation of their associated pathways, with a yet uncertain role for the BBB (Figure 8). Although CLR1404 can also be labeled with ^{131}I for therapeutic options, mild uptake in benign treatment-related brain parenchymal changes may lower specificity of this agent and limit its (theragnostic) use (153-155). ^{18}F-ML-10 enters apoptotic cells that are characterized by externalized phosphatidylserine (PS) and an intact plasma membrane (Figure 8), features not present in necrotic, dying cells. The agent does not seem to cross the intact BBB. In clinical practice, uptake will therefore likely reflect BBB permeability +/- increased apoptotic rates. High apoptotic rates, however, are common in both tumor tissue and tissue treated with radiotherapy or e.g., ischemia, decreasing tumor specificity of this agent as well (156). $^{64}CuCl_2$ enters cells through the Ctr1 copper transporter after which it becomes directly incorporated into cellular pathways in the same way as Cu^+ released from $^{62}Cu^{2+}$-ATSM (Figure 8). The agent has the added advantage of being both a diagnostic agent (β^+ decay) and a therapeutic agent (Auger electrons). Nonetheless, how $^{64}CuCl_2$ crosses the BBB, if it does at all, is not known yet, and its use has remained limited to two somewhat older clinical studies (157).

Miscellaneous agents

For some additional agents, uptake mechanisms are less clear. ^{11}C-TGN-020 is a ligand for aquaporins (AQP) 1 and 4, water channel proteins that play a role in cerebrospinal fluid absorption and regulation of BBB permeability; in brain tumors they stimulate angiogenesis, BBB permeability, tumor cell

migration and invasion (Figure 1 and Figure 7) (158). AQPs are only present on dural and vascular membranes and neurons (Table 3), causing low healthy brain uptake of ^{11}C-TGN-020 (**Figure 9**). The role of AQPs in tumor invasion and microvascular proliferation suggests ^{11}C-TGN-020 could improve differentiation between tumor grades (Figure 9); however, so far only WHO grade III and IV astrocytomas have been studied (159). If and how this agent crosses the BBB is not known yet, although AQPs have been described next to the BBB (Table 3). ^{68}Ga-citrate binds to transferrin in blood, and this complex subsequently binds to the transferrin receptor TFRC after which it most likely becomes endocytosed (Figure 7) (160). TFRC plays an essential part in iron homeostasis, is often overexpressed on brain tumor cells (at least partly because of MYC overexpression) and thought to stimulate multiple tumor cellular pathways by supplying the necessary increased amounts of iron as building block (Figure 1) (161). Tumor specificity, whether the agent crosses the BBB, and what happens after the ^{68}Ga-citrate-transferrin complex is endocytosed inside the cell however remain to be seen (160).

Fibroblast activation protein (FAP) inhibitor (FAPI) PET imaging using ^{68}Ga-(DOTA)-FAPI or ^{18}F-FAPI is only recently being explored. FAP is a cell membrane-bound glycoprotein with serine protease activity that can cleave proteins in the surrounding tissue allowing for protein degradation and matrix remodeling. In tumors, it promotes cellular proliferation, migration and invasion, angiogenesis, and immune suppression through several pathways, not all of which have been completely elucidated (Figure 1 and Figure 7). It is generally absent or shows very low expression in normal cells, but is a universal marker of tumor-associated fibroblasts (162). In extracranial tumors, ^{68}Ga-(DOTA)-FAPI and ^{18}F-FAPI can target these fibroblast within the tumor microenvironment (163). Fibroblasts are not present in brain (tumors); however, it does appear that there are FAP-positive cells such as FAP-positive foci of neoplastic cells in gliomas and FAP-positive vessels in glial tumors, and FAP seems to be overexpressed in most glioblastomas. Neither agent crosses the BBB, so uptake in clinical practice will reflect at least BBB permeability, possibly combined with FAP overexpression (164). One advantage is that FAPI agents have low background activity in the brain parenchyma (165). There is some initial evidence suggesting that FAPI agents may be helpful in distinguishing between low-grade IDH-mutant and high-grade gliomas (166).

^{68}Ga-Pentixafor targets C-X-C motif chemokine receptor 4 (CXCR4). CXCR4 is a transmembrane receptor that is involved in multiple physiological processes such as embryogenesis, neoangiogenesis, hematopoiesis and inflammation. In tumors, the interaction of CXCR4 and its ligand CXCL12 (C-X-C motif chemokine ligand) plays a critical role in tumor cell growth and survival, angiogenesis, and

regulation of interactions between tumor cells and the TME (Figure 7) (167). The receptor is overexpressed in numerous human tumor types, including glioblastoma and lymphoma, and is associated with poorer progression-free survival and overall survival (168). Recent studies have demonstrated ^{68}Ga-Pentixafor uptake in glioblastoma and primary central nervous system lymphoma on PET and the agent may have therapeutic potential if labelled with ^{177}Lu or ^{90}Y (169, 170). A recent histopathologic study on glioblastoma tissue samples, however, showed a large inter- and even intra-tumoral variation in CXCR4 expression, and an inconsistent correlation between *ex vivo* CXCR4 expression and *in vivo* uptake of ^{68}Ga-Pentixafor (171). In addition, the agent cannot cross the intact BBB. These factors bear the question to what extent uptake reflects BBB permeability versus CXCR4 overexpression.

^{82}Rb-chloride is an analog of potassium and enters cells through the sodium-potassium pump or Na/K-ATPase found ubiquitously in human cells as well as tumor cells. Next to maintaining cellular ionic homeostasis, the Na/K-ATPase is also involved in many intracellular pathways affecting cellular proliferation, motility and apoptosis; in glioblastomas its overexpression sustains growth and invasion (Figure 8) (172). Although the agent can penetrate the BBB from extracellular fluid, uptake does depend on BBB integrity since no uptake is seen in healthy brain parenchyma. After entering cells, retention depends at least partly on ATP-driven transport of the Na/K-ATPase. In clinical practice, uptake will therefore likely reflect a combination of vascularization rate, BBB permeability, and efficiency of Na/K-ATPase (173). All three of these factors are often higher in malignant tumors as compared to benign tumors, which may allow for differentiation between malignant and benign gliomas. However, due to its non-specificity, ^{82}Rb-chloride uptake can be seen in both tumors and other lesions such as AVMs (174).

PET AGENTS 'INCIDENTALLY' FOUND TO ACCUMULATE IN BRAIN TUMORS

Three agents were initially developed for imaging of other pathologic processes such as inflammation (^{18}F-FDS), Parkinson's disease (^{18}F-FP-CIT) and Alzheimer's disease (^{11}C-PiB). Their mechanisms of interaction and assimilation within brain tumor cells are unclear, and data on brain tumor uptake is limited to case reports. ^{18}F-FDS showed uptake in spindle cell carcinoma of the pituitary gland, although the confounding effect of BBB leakage in this case was unclear (175). ^{18}F-FP-CIT has shown uptake in meningiomas, although the cause of its uptake and role of the dopamine active transporter (DAT) in meningioma oncogenesis is still unknown(176). ^{11}C-PiB binds β-amyloid in PET-imaging of Alzheimer's disease but has also shown uptake in meningiomas. A lack of uptake in other tumors suggests ^{11}C-PiB may be able to differentiate between meningiomas and other brain tumor types;

however, the general absence or minimal presence of β-amyloid within meningioma suggests uptake might primarily be due to high vascularity (177).

CONCLUSION

Interpretation of PET agent uptake in brain tumors remains complex. This is due in part to the various factors influencing uptake, such as transporter / receptor expression in non-tumorous tissues, BBB permeability, and metabolic incorporation versus 'inactive' trapping. For many agents, these factors have not been completely elucidated. In addition, knowledge on oncogenesis improves rapidly, shedding new light on brain tumor development and emphasizing molecular pathways that are not targeted by existing PET agents. Finally, although the Response Assessment in Neuro-Oncology working group (RANO) published guidelines for the use of a few common PET agents for glioma imaging, many countries allow PET agents that have been used in clinical studies to be synthesized and used in the associated institution's clinical practice, as long as the institution can substantiate it may improve patient care, increasing exposure of clinical radiologists to these often less well-known PET agents.(178) We hope that this monograph of PET agents used for human brain tumors has contributed to a better understanding of uptake mechanisms and their clinical implications. None of the PET agents described have been shown to be the 'ideal', tumor-specific agent. Perhaps in the future, simultaneous PET/MRI, combining the advantages of conventional and molecular MR imaging with targeted PET imaging, could prove the optimal combination for brain tumor diagnosis, treatment monitoring and follow-up.

CONFLICT OF INTEREST

The authors declare no potential conflict of interest with respect to research, authorship and/or publication of this article.

COPYRIGHT AND PERMISSION STATEMENT

Copyright and Permission Statement: The authors confirm that the materials included in this chapter do not violate copyright laws. Where relevant, appropriate permissions have been obtained from the original copyright holder(s), and all original sources have been appropriately acknowledged or referenced. Where relevant, informed consent has been obtained from patients or their caregivers according to applicable national or institutional policies.

REFERENCES

1. Stupp R, Mason WP, van den Bent MJ, Weller M, Fisher B, Taphoorn MJ, et al. Radiotherapy plus concomitant and adjuvant temozolomide for glioblastoma. N Eng J Med 2005;352(10):987-996
https://doi.org/10.1056/NEJMoa043330

2. Louis DN, Perry A, Wesseling P, Brat DJ, Cree IA, Figarella-Branger D, et al. The 2021 WHO Classification of Tumors of the Central Nervous System: a summary. Neuro Oncol 2021;23(8):1231-1251
https://doi.org/10.1093/neuonc/noab106

3. Langen KJ, Galldiks N, Hattingen E, Shah NJ. Advances in neuro-oncology imaging. Nat Rev Neurol 2017;13(5):279-289
https://doi.org/10.1038/nrneurol.2017.44

4. Kim MM, Parolia A, Dunphy MP, Venneti S. Non-invasive metabolic imaging of brain tumours in the era of precision medicine. Nat Rev Clin Oncol 2016;13(12):725-739
https://doi.org/10.1038/nrclinonc.2016.108

5. Werner JM, Lohmann P, Fink GR, Langen KJ, Galldiks N. Current Landscape and Emerging Fields of PET Imaging in Patients with Brain Tumors. Molecules 2020;25(6):1471
https://doi.org/10.3390/molecules25061471

6. Borja AJ, Hancin EC, Raynor WY, Ayubcha C, Detchou DK, Werner TJ, et al. A Critical Review of PET Tracers Used for Brain Tumor Imaging. PET Clin 2021;16(2):219-231
https://doi.org/10.1016/j.cpet.2020.12.004

7. Verger A, Kas A, Darcourt J, Guedj E. PET Imaging in Neuro-Oncology: An Update and Overview of a Rapidly Growing Area. Cancers 2022;14(5):1103
https://doi.org/10.3390/cancers14051103

8. Weinberg RA. Coming full circle-from endless complexity to simplicity and back again. Cell 2014;157(1):267-271
https://doi.org/10.1016/j.cell.2014.03.004

9. Fouad YA, Aanei C. Revisiting the hallmarks of cancer. Am J Cancer Res 2017;7(5):1016-1036

10. Strickland M, Stoll EA. Metabolic Reprogramming in Glioma. Front Cell Dev Biol 2017;5:43
https://doi.org/10.3389/fcell.2017.00043

11. Pang LY, Hurst EA, Argyle DJ. Cyclooxygenase-2: A Role in Cancer Stem Cell Survival and Repopulation of Cancer Cells during Therapy. Stem Cells Int 2016;2016:2048731
https://doi.org/10.1155/2016/2048731

12. Kalkat M, De Melo J, Hickman KA, Lourenco C, Redel C, Resetca D, et al. MYC Deregulation in Primary Human Cancers. Genes 2017;8(6):151
https://doi.org/10.3390/genes8060151

13. Dejure FR, Eilers M. MYC and tumor metabolism: chicken and egg. EMBO J 2017;36(23):3409-3420
https://doi.org/10.15252/embj.201796438

14. Swartling FJ. Myc proteins in brain tumor development and maintenance. Ups J Med Sci 2012;117(2):122-131
https://doi.org/10.3109/03009734.2012.658975

15. Hede SM, Nazarenko I, Nister M, Lindstrom MS. Novel Perspectives on p53 Function in Neural Stem Cells and Brain Tumors. J Oncol 2011;2011:852970
https://doi.org/10.1155/2011/852970

16. Colman HA, K. Molecular Pathogenesis. In: P. NARDW, ed. Primary Central Nervous System Tumors Current Clinical Oncology: Humana Press, 2011; p. 27-44
https://doi.org/10.1007/978-1-60761-166-0_2

17. Shi D, Gu W. Dual Roles of MDM2 in the Regulation of p53: Ubiquitination Dependent and Ubiquitination Independent Mechanisms of MDM2 Repression of p53 Activity. Genes Cancer 2012;3(3-4):240-248
https://doi.org/10.1177/1947601912455199

18. LaPak KM, Burd CE. The molecular balancing act of p16(INK4a) in cancer and aging. Mol Cancer Res 2014;12(2):167-183
https://doi.org/10.1158/1541-7786.MCR-13-0350

19. Dick FA, Rubin SM. Molecular mechanisms underlying RB protein function. Nat Rev Mol Cell Biol 2013;14(5):297-306
https://doi.org/10.1038/nrm3567

20. Hegi ME, Diserens AC, Gorlia T, Hamou MF, de Tribolet N, Weller M, et al. MGMT gene silencing and benefit from temozolomide in glioblastoma. New Eng J Med 2005;352(10):997-1003
https://doi.org/10.1056/NEJMoa043331

21. Louis DN, Perry A, Reifenberger G, von Deimling A, Figarella-Branger D, Cavenee WK, et al. The 2016 World Health Organization Classification of Tumors of the Central Nervous System: a summary. Acta Neuropathol 2016;131(6):803-820
https://doi.org/10.1007/s00401-016-1545-1

22. Waitkus MS, Diplas BH, Yan H. Isocitrate dehydrogenase mutations in gliomas. Neuro Oncol 2016;18(1):16-26
https://doi.org/10.1093/neuonc/nov136

23. Jafri MA, Ansari SA, Alqahtani MH, Shay JW. Roles of telomeres and telomerase in cancer, and advances in telomerase-targeted therapies. Genome Med 2016;8(1):69
https://doi.org/10.1186/s13073-016-0324-x

24. Lv L, Zhang Y, Zhao Y, Wei Q, Zhao Y, Yi Q. Effects of 1p/19q Codeletion on Immune Phenotype in Low Grade Glioma. Front Cell Neurosci 2021;15:704344
https://doi.org/10.3389/fncel.2021.704344

25. Dagogo-Jack I, Shaw AT. Tumour heterogeneity and resistance to cancer therapies. Nat Rev Clin Oncol 2018;15(2):81-94
https://doi.org/10.1038/nrclinonc.2017.166

26. DeBerardinis RJ, Chandel NS. Fundamentals of cancer metabolism. Sci Adv 2016;2(5):e1600200
https://doi.org/10.1126/sciadv.1600200

27. Park JW. Metabolic Rewiring in Adult-Type Diffuse Gliomas. Int J Mol Sci 2023;24(8):7348
https://doi.org/10.3390/ijms24087348

28. Park SH, Won J, Kim SI, Lee Y, Park CK, Kim SK, et al. Molecular Testing of Brain Tumor. J Pathol Transl Med 2017;51(3):205-223
https://doi.org/10.4132/jptm.2017.03.08

29. Yang L, Venneti S, Nagrath D. Glutaminolysis: A Hallmark of Cancer Metabolism. Annu Rev Biomed Eng 2017;19:163-194
https://doi.org/10.1146/annurev-bioeng-071516-044546

30. Liberti MV, Locasale JW. The Warburg Effect: How Does it Benefit Cancer Cells? Trends Biochem Sci 2016;41(3):211-218
https://doi.org/10.1016/j.tibs.2015.12.001

31. Romero-Garcia S, Moreno-Altamirano MM, Prado-Garcia H, Sanchez-Garcia FJ. Lactate Contribution to the Tumor Microenvironment: Mechanisms, Effects on Immune Cells and Therapeutic Relevance. Front Immunol 2016;7:52
https://doi.org/10.3389/fimmu.2016.00052

32. San-Millan I, Brooks GA. Reexamining cancer metabolism: lactate production for carcinogenesis could be the purpose and explanation of the Warburg Effect. Carcinogenesis 2017;38(2):119-133
https://doi.org/10.1093/carcin/bgw127

33. Tsuchihashi K, Okazaki S, Ohmura M, Ishikawa M, Sampetrean O, Onishi N, et al. The EGF Receptor Promotes the Malignant Potential of Glioma by Regulating Amino Acid Transport System xc(-). Cancer Res 2016;76(10):2954-2963
https://doi.org/10.1158/0008-5472.CAN-15-2121

34. Nussenbaum F, Herman IM. Tumor angiogenesis: insights and innovations. JJ Oncol 2010;2010:132641
https://doi.org/10.1155/2010/132641

35. De Palma M, Biziato D, Petrova TV. Microenvironmental regulation of tumour angiogenesis. Nat Rev Cancer 2017;17(8):457-474
https://doi.org/10.1038/nrc.2017.51

36. Hardee ME, Zagzag D. Mechanisms of glioma-associated neovascularization. Am J Pathol 2012;181(4):1126-1141
https://doi.org/10.1016/j.ajpath.2012.06.030

37. Petrova V, Annicchiarico-Petruzzelli M, Melino G, Amelio I. The hypoxic tumour microenvironment. Oncogenesis 2018;7(1):10
https://doi.org/10.1038/s41389-017-0011-9

38. Beppu TS, Sato Y, Terasaki K. High-Uptake Areas on 18F-FRP170 PET Image Necessarily Include Proliferating Areas in Glioblastoma: A Superimposed Image Study Combining 18F-FRP170 PET with 11C-methionine PET. Adv Mol Imaging 2017;7:11
https://doi.org/10.4236/ami.2017.71001

39. Muz B, de la Puente P, Azab F, Azab AK. The role of hypoxia in cancer progression, angiogenesis, metastasis, and resistance to therapy. Hypoxia 2015;3:83-92
https://doi.org/10.2147/HP.S93413

40. Hirata K, Yamaguchi S, Shiga T, Kuge Y, Tamaki N. The Roles of Hypoxia Imaging Using (18)F-Fluoromisonidazole Positron Emission Tomography in Glioma Treatment. J Clin Med 2019;8(8):1088
https://doi.org/10.3390/jcm8081088

41. Goel HL, Mercurio AM. VEGF targets the tumour cell. Nat Rev Cancer 2013;13(12):871-882
https://doi.org/10.1038/nrc3627

42. Belli C, Trapani D, Viale G, D'Amico P, Duso BA, Della Vigna P, et al. Targeting the microenvironment in solid tumors. Cancer Treat Rev 2018;65:22-32
https://doi.org/10.1016/j.ctrv.2018.02.004

43. Labak CM, Wang PY, Arora R, Guda MR, Asuthkar S, Tsung AJ, et al. Glucose transport: meeting the metabolic demands of cancer, and applications in glioblastoma treatment. Am J Cancer Res 2016;6(8):1599-1608

44. Kim D, Kim S, Kim SH, Chang JH, Yun M. Prediction of Overall Survival Based on Isocitrate Dehydrogenase 1 Mutation and 18F-FDG Uptake on PET/CT in Patients With Cerebral Gliomas. Clin Nucl Med 2018;43(5):311-316
https://doi.org/10.1097/RLU.0000000000002006

45. Withofs N, Kumar R, Alavi A, Hustinx R. Facts and Fictions About [(18)F]FDG versus Other Tracers in Managing Patients with Brain Tumors: It Is Time to Rectify the Ongoing Misconceptions. PET Clin 2022;17(3):327-342
https://doi.org/10.1016/j.cpet.2022.03.004

46. Kong Z, Li J, Liu Z, Liu Z, Zhao D, Cheng X, et al. Radiomics signature based on FDG-PET predicts proliferative activity in primary glioma. Clin Radiol 2019;74(10): e815-e823
https://doi.org/10.1016/j.crad.2019.06.019

47. Mansoor NM, Thust S, Militano V, Fraioli F. PET imaging in glioma: techniques and current evidence. Nucl Med Comm 2018;39(12):1064-1080
https://doi.org/10.1097/MNM.0000000000000914

48. Kepe V, Scafoglio C, Liu J, Yong WH, Bergsneider M, Huang SC, et al. Positron emission tomography of sodium glucose cotransport activity in high grade astrocytomas. J Neurooncol 2018;138(3):557-569
https://doi.org/10.1007/s11060-018-2823-7

49. Oka S, Okudaira H, Ono M, Schuster DM, Goodman MM, Kawai K, et al. Differences in transport mechanisms of trans-1-amino-3-[18F]fluorocyclobutanecarboxylic acid in inflammation, prostate cancer, and glioma cells: comparison with L-[methyl-11C]methionine and 2-deoxy-2-[18F]fluoro-D-glucose. Mol Imaging Biol 2014;16(3):322-329
https://doi.org/10.1007/s11307-013-0693-0

50. Kandasamy P, Gyimesi G, Kanai Y, Hediger MA. Amino acid transporters revisited: New views in health and disease. Trends Biochem Sci 2018;43(10):752-789
https://doi.org/10.1016/j.tibs.2018.05.003

51. Haining Z, Kawai N, Miyake K, Okada M, Okubo S, Zhang X, et al. Relation of LAT1/4F2hc expression with pathological grade, proliferation and angiogenesis in human gliomas. BMC Clin Pathol 2012;12:4
https://doi.org/10.1186/1472-6890-12-4

52. Parent EE, Benayoun M, Ibeanu I, Olson JJ, Hadjipanayis CG, Brat DJ, et al. [(18)F]Fluciclovine PET discrimination between high- and low-grade gliomas. EJNMMI Res 2018;8(1):67
https://doi.org/10.1186/s13550-018-0415-3

53. Sun A, Liu X, Tang G. Carbon-11 and Fluorine-18 Labeled Amino Acid Tracers for Positron Emission Tomography Imaging of Tumors. Front Chem 2017;5:124
https://doi.org/10.3389/fchem.2017.00124

54. Deng H, Tang X, Wang H, Tang G, Wen F, Shi X, et al. S-11C-methyl-L-cysteine: a new amino acid PET tracer for cancer imaging. J Nucl Med 2011;52(2):287-293
https://doi.org/10.2967/jnumed.110.081349

55. de Wolde H, Pruim J, Mastik MF, Koudstaal J, Molenaar WM. Proliferative activity in human brain tumors: comparison of histopathology and L-[1-(11)C]tyrosine PET. J Nucl Med 1997;38(9):1369-1374

56. Nakajima R, Kimura K, Abe K, Sakai S. (11)C-methionine PET/CT findings in benign brain disease. Jpn J Radiol 2017;35(6):279-288
https://doi.org/10.1007/s11604-017-0638-7

57. Dadone-Montaudie B, Ambrosetti D, Dufour M, Darcourt J, Almairac F, Coyne J, et al. [18F] FDOPA standardized uptake values of brain tumors are not exclusively dependent on LAT1 expression. PloS One 2017;12(9):e0184625
https://doi.org/10.1371/journal.pone.0184625

58. Horiguchi K, Tosaka M, Higuchi T, Arisaka Y, Sugawara K, Hirato J, et al. Clinical value of fluorine-18alpha-methyltyrosine PET in patients with gliomas: comparison with fluorine-18 fluorodeoxyglucose PET. EJNMMI Res 2017;7(1):50
https://doi.org/10.1186/s13550-017-0298-8

59. Moon H, Byun BH, Lim I, Kim BI, Choi CW, Rhee CH, et al. A Phase 0 Microdosing PET/CT Study Using O-[18F]Fluoromethyl-d-Tyrosine in Normal Human Brain and Brain Tumor. Clin Nucl Med 2021;46(9):717-722
https://doi.org/10.1097/RLU.0000000000003735

60. Cicone F, Filss CP, Minniti G, Rossi-Espagnet C, Papa A, Scaringi C, et al. Volumetric assessment of recurrent or progressive gliomas: comparison between F-DOPA PET and perfusion-weighted MRI. Eur J Nucl Med Mol Imaging 2015;42(6):905-915
https://doi.org/10.1007/s00259-015-3018-5

61. Roach JR, Plaha P, McGowan DR, Higgins GS. The role of [(18)F]fluorodopa positron emission tomography in grading of gliomas. J Neurooncol 2022;160(3):577-589
https://doi.org/10.1007/s11060-022-04177-3

62. Renard D, Collombier L, Laurent-Chabalier S, Mura T, Le Floch A, Fertit HE, et al. (18)F-FDOPA-PET in pseudotumoral brain lesions. J Neurol 2021;268(4):1266-1275
https://doi.org/10.1007/s00415-020-10269-9

63. Nozaki S, Nakatani Y, Mawatari A, Hume WE, Wada Y, Ishii A, et al. First-in-human assessment of the novel LAT1 targeting PET probe (18)F-FIMP. Biochem Biophys Res Comm 2022;596:83-87
https://doi.org/10.1016/j.bbrc.2022.01.099

64. Nozaki S, Nakatani Y, Mawatari A, Shibata N, Hume WE, Hayashinaka E, et al. (18)F-FIMP: a LAT1-specific PET probe for discrimination between tumor tissue and inflammation. Sci Rep 2019;9(1):15718
https://doi.org/10.1038/s41598-019-52270-x

65. Hawkins RA, O'Kane RL, Simpson IA, Viña JR. Structure of the blood-brain barrier and its role in the transport of amino acids. J Nutr 2006;136(1 Suppl):218s-226s
https://doi.org/10.1093/jn/136.1.218S

66. Parente A, van Waarde A, Shoji A, de Paula Faria D, Maas B, Zijlma R, et al. PET Imaging with S-[(11)C]Methyl-L-Cysteine and L-[Methyl-(11)C]Methionine in Rat Models of Glioma, Glioma Radiotherapy, and Neuroinflammation. Mol Imaging Biol 2018;20(3):465-472
https://doi.org/10.1007/s11307-017-1137-z

67. Langen KJ, Stoffels G, Filss C, Heinzel A, Stegmayr C, Lohmann P, et al. Imaging of amino acid transport in brain tumours: Positron emission tomography with O-(2-[(18)F]fluoroethyl)-L-tyrosine (FET). Methods 2017;130:124-134
https://doi.org/10.1016/j.ymeth.2017.05.019

68. Calcagni ML, Galli G, Giordano A, Taralli S, Anile C, Niesen A, et al. Dynamic O-(2-[18F]fluoroethyl)-L-tyrosine (F-18 FET) PET for glioma grading: assessment of individual probability of malignancy. Clin Nucl Med 2011;36(10):841-847
https://doi.org/10.1097/RLU.0b013e3182291b40

69. Jansen NL, Suchorska B, Wenter V, Schmid-Tannwald C, Todica A, Eigenbrod S, et al. Prognostic significance of dynamic 18F-FET PET in newly diagnosed astrocytic high-grade glioma. J Nucl Med 2015;56(1):9-15
https://doi.org/10.2967/jnumed.114.144675

70. Stegmayr C, Stoffels G, Filß C, Heinzel A, Lohmann P, Willuweit A, et al. Current trends in the use of O-(2-[(18)F]fluoroethyl)-L-tyrosine ([(18)F]FET) in neurooncology. Nucl Med Biol 2021;92:78-84
https://doi.org/10.1016/j.nucmedbio.2020.02.006

71. Juhasz C, Muzik O, Chugani DC, Chugani HT, Sood S, Chakraborty PK, et al. Differential kinetics of alpha-[(1)(1)C]methyl-L-tryptophan on PET in low-grade brain tumors. J Neurooncol 2011;102(3):409-415
https://doi.org/10.1007/s11060-010-0327-1

72. John F, Bosnyák E, Robinette NL, Amit-Yousif AJ, Barger GR, Shah KD, et al. Multimodal imaging-defined subregions in newly diagnosed glioblastoma: impact on overall survival. Neuro Oncol 2019;21(2):264-273
https://doi.org/10.1093/neuonc/noy169

73. Kamson DO, Mittal S, Buth A, Muzik O, Kupsky WJ, Robinette NL, et al. Differentiation of glioblastomas from metastatic brain tumors by tryptophan uptake and kinetic analysis: a positron emission tomographic study with magnetic resonance imaging comparison. Mol Imaging 2013;12(5):327-337
https://doi.org/10.2310/7290.2013.00048

74. Alkonyi B, Barger GR, Mittal S, Muzik O, Chugani DC, Bahl G, et al. Accurate differentiation of recurrent gliomas from radiation injury by kinetic analysis of alpha-11C-methyl-L-tryptophan PET. J Nucl Med 2012;53(7):1058-1064
https://doi.org/10.2967/jnumed.111.097881

75. Takahashi Y, Imahori Y, Mineura K. Prognostic and therapeutic indicator of fluoroboronophenylalanine positron emission tomography in patients with gliomas. Clin Cancer Res 2003;9(16 Pt 1):5888-5895

76. Lo YW, Lee JC, Hu YS, Li CY, Chen YL, Lin CS, et al. The importance of optimal ROIs delineation for FBPA-PET before BNCT. Appl Radiat Isot 2020;163:109219
https://doi.org/10.1016/j.apradiso.2020.109219

77. Watabe T, Ikeda H, Nagamori S, Wiriyasermkul P, Tanaka Y, Naka S, et al. (18)F-FBPA as a tumor-specific probe of L-type amino acid transporter 1 (LAT1): a comparison study with (18)F-FDG and (11)C-Methionine PET. Eur J Nucl Med Mol Imaging 2017;44(2):321-331
https://doi.org/10.1007/s00259-016-3487-1

78. Kong Z, Li Z, Chen J, Liu S, Liu D, Li J, et al. Metabolic characteristics of [(18)F]fluoroboronotyrosine (FBY) PET in malignant brain tumors. Nucl Med Biol 2022;106-107:80-87
https://doi.org/10.1016/j.nucmedbio.2022.01.002

79. Kong Z, Li Z, Chen J, Ma W, Wang Y, Yang Z, et al. Larger (18)F-fluoroboronotyrosine (FBY) active volume beyond MRI contrast enhancement in diffuse gliomas than in circumscribed brain tumors. EJNMMI Res 2022;12(1):22
https://doi.org/10.1186/s13550-022-00896-w

80. Tsuyuguchi N, Terakawa Y, Uda T, Nakajo K, Kanemura Y. Diagnosis of Brain Tumors Using Amino Acid Transport PET Imaging with (18)F-fluciclovine: A Comparative Study with L-methyl-(11)C-methionine PET Imaging. Asia Ocean J Nucl Med Biol 2017;5(2):85-94

81. Venneti S, Dunphy MP, Zhang H, Pitter KL, Zanzonico P, Campos C, et al. Glutamine-based PET imaging facilitates enhanced metabolic evaluation of gliomas in vivo. Sci Transl Med 2015;7(274):274ra217
https://doi.org/10.1126/scitranslmed.aaa1009

82. Albano D, Tomasini D, Bonù M, Giubbini R, Bertagna F. (18)F-Fluciclovine ((18)F-FACBC) PET/CT or PET/MRI in gliomas/glioblastomas. Ann Nucl Med 2020;34(2):81-86
https://doi.org/10.1007/s12149-019-01426-w

83. Mittra ES, Koglin N, Mosci C, Kumar M, Hoehne A, Keu KV, et al. Pilot Preclinical and Clinical Evaluation of (4S)-4-(3-[18F]Fluoropropyl)-L-Glutamate (18F-FSPG) for PET/CT Imaging of Intracranial Malignancies. PloS One 2016;11(2):e0148628
https://doi.org/10.1371/journal.pone.0148628

84. Wardak M, Sonni I, Fan AP, Minamimoto R, Jamali M, Hatami N, et al. (18)F-FSPG PET/CT Imaging of System x(C)(-) Transporter Activity in Patients with Primary and Metastatic Brain Tumors. Radiology 2022;303(3):620-631
https://doi.org/10.1148/radiol.203296

85. Verger A, Stoffels G, Galldiks N, Lohmann P, Willuweit A, Neumaier B, et al. Investigation of cis-4-[(18)F]Fluoro-D-Proline Uptake in Human Brain Tumors After Multimodal Treatment. Mol Imaging Biol 2018;20(6):1035-1043
https://doi.org/10.1007/s11307-018-1197-8

86. Nishii R, Higashi T, Kagawa S, Arimoto M, Kishibe Y, Takahashi M, et al. Differential Diagnosis between Low-Grade and High-Grade Astrocytoma Using System A Amino Acid Transport PET Imaging with C-11-MeAIB: A Comparison Study with C-11-Methionine PET Imaging. Contrast Media Mol Imaging 2018;2018:1292746
https://doi.org/10.1155/2018/1292746

87. Kagawa S, Nishii R, Higashi T, Yamauchi H, Ogawa E, Okudaira H, et al. Relationship between [(14)C]MeAIB uptake and amino acid transporter family gene expression levels or proliferative activity in a pilot study in human carcinoma cells: Comparison with [(3)H]methionine uptake. Nucl Med Biol 2017;49:8-15
https://doi.org/10.1016/j.nucmedbio.2017.01.008

88. Zaragozá R. Transport of Amino Acids Across the Blood-Brain Barrier. Front Physiol 2020;11:973
https://doi.org/10.3389/fphys.2020.00973

89. Machova E, O'Regan S, Newcombe J, Meunier FM, Prentice J, Dove R, et al. Detection of choline transporter-like 1 protein CTL1 in neuroblastoma x glioma cells and in the CNS, and its role in choline uptake. J Neurochem 2009;110(4):1297-1309
https://doi.org/10.1111/j.1471-4159.2009.06218.x

90. Arlauckas SP, Popov AV, Delikatny EJ. Choline kinase alpha-Putting the ChoK-hold on tumor metabolism. Prog Lipid Res 2016;63:28-40
https://doi.org/10.1016/j.plipres.2016.03.005

91. Shinoura N, Nishijima M, Hara T, Haisa T, Yamamoto H, Fujii K, et al. Brain tumors: detection with C-11 choline PET. Radiology 1997;202(2):497-503
https://doi.org/10.1148/radiology.202.2.9015080

92. Tian M, Zhang H, Oriuchi N, Higuchi T, Endo K. Comparison of 11C-choline PET and FDG PET for the differential diagnosis of malignant tumors. Eur J Nucl Med Mol Imaging 2004;31(8):1064-1072
https://doi.org/10.1007/s00259-004-1496-y

93. Mertens K, Ham H, Deblaere K, Kalala JP, Van den Broecke C, Slaets D, et al. Distribution patterns of 18F-labelled fluoromethylcholine in normal structures and tumors of the head: a PET/MRI evaluation. Clin Nucl Med 2012;37(8):e196-203
https://doi.org/10.1097/RLU.0b013e31824c5dd0

94. Huang Z, Zuo C, Guan Y, Zhang Z, Liu P, Xue F, et al. Misdiagnoses of 11C-choline combined with 18F-FDG PET imaging in brain tumours. Nucl Med Comm 2008;29(4):354-358
https://doi.org/10.1097/MNM.0b013e3282f4a21e

95. García Vicente AM, Pena Pardo FJ, Lozano Setien E, Sandoval Valencia H, Villena Martín M. FuMeGA Criteria for Visual Assessment of Postoperative 18F-Fluorocholine PET in Patients With Glioma. Clin Nucl Med 2020;45(6):448-450
https://doi.org/10.1097/RLU.0000000000003034

96. Ferrazzoli V, Shankar A, Cockle JV, Tang C, Al-Khayfawee A, Bomanji J, et al. Mapping glioma heterogeneity using multiparametric 18 F-choline PET/MRI in childhood and teenage-young adults. Nucl Med Comm 2023;44(1):91-99
https://doi.org/10.1097/MNM.0000000000001636

97. Kim S, Kim D, Kim SH, Park MA, Chang JH, Yun M. The roles of (11)C-acetate PET/CT in predicting tumor differentiation and survival in patients with cerebral glioma. Eur J Nucl Med Mol Imaging 2018;45(6):1012-1020
https://doi.org/10.1007/s00259-018-3948-9

98. Liu RS, Chang CP, Guo WY, Pan DH, Ho DM, Chang CW, et al. 1-11C-acetate versus 18F-FDG PET in detection of meningioma and monitoring the effect of gamma-knife radiosurgery. J Nucl Med 2010;51(6):883-891
https://doi.org/10.2967/jnumed.109.070565

99. Bhowmik A, Khan R, Ghosh MK. Blood brain barrier: a challenge for effectual therapy of brain tumors. BioMed Res Int 2015;2015:320941
https://doi.org/10.1155/2015/320941

100. Schug ZT, Vande Voorde J, Gottlieb E. The metabolic fate of acetate in cancer. Nat Rev Cancer 2016;16(11):708-717
https://doi.org/10.1038/nrc.2016.87

101. Shi X, Liu Y, Zhang X, Yi C, Wang X, Chen Z, Zhang B. The comparison of 13N-ammonia and 18F-FDG in the evaluation of untreated gliomas. Clin Nucl Med 2013;38(7):522-526
https://doi.org/10.1097/RLU.0b013e318295298d

102. Beinat C, Patel CB, Haywood T, Shen B, Naya L, Gandhi H, et al. Human biodistribution and radiation dosimetry of [(18)F]DASA-23, a PET probe targeting pyruvate kinase M2. Eur J Nucl Med Mol Imaging 2020;47(9):2123-2130
https://doi.org/10.1007/s00259-020-04687-0

103. Su Q, Luo S, Tan Q, Deng J, Zhou S, Peng M, et al. The role of pyruvate kinase M2 in anticancer therapeutic treatments. Oncol Lett 2019;18(6):5663-5672
https://doi.org/10.3892/ol.2019.10948

104. Beinat C, Patel CB, Haywood T, Murty S, Naya L, Castillo JB, et al. A Clinical PET Imaging Tracer ([(18)F]DASA-23) to Monitor Pyruvate Kinase M2-Induced Glycolytic Reprogramming in Glioblastoma. Clin Cancer Res 2021;27(23):6467-6478
https://doi.org/10.1158/1078-0432.CCR-21-0544

105. Choi SJ, Kim JS, Kim JH, Oh SJ, Lee JG, Kim CJ, et al. [18F]3'-deoxy-3'-fluorothymidine PET for the diagnosis and grading of brain tumors. Eur J Nucl Med Mol Imaging 2005;32(6):653-659
https://doi.org/10.1007/s00259-004-1742-3

106. Shinomiya A, Kawai N, Okada M, Miyake K, Nakamura T, Kushida Y, et al. Evaluation of 3'-deoxy-3'-[18F]-fluorothymidine (18F-FLT) kinetics correlated with thymidine kinase-1 expression and cell proliferation in newly diagnosed gliomas. Eur J Nucl Med Mol Imaging 2013;40(2):175-185
https://doi.org/10.1007/s00259-012-2275-9

107. Nowosielski M, DiFranco MD, Putzer D, Seiz M, Recheis W, Jacobs AH, et al. An intra-individual comparison of MRI, [18F]-FET and [18F]-FLT PET in patients with high-grade gliomas. PloS One 2014;9(4):e95830
https://doi.org/10.1371/journal.pone.0095830

108. Nikaki A, Angelidis G, Efthimiadou R, Tsougos I, Valotassiou V, Fountas K, et al. (18)F-fluorothymidine PET imaging in gliomas: an update. Ann Nucl Med 2017;31(7):495-505
https://doi.org/10.1007/s12149-017-1183-2

109. Collet S, Guillamo JS, Berro DH, Chakhoyan A, Constans JM, Lechapt-Zalcman E, et al. Simultaneous Mapping of Vasculature, Hypoxia, and Proliferation Using Dynamic Susceptibility Contrast MRI, (18)F-FMISO PET, and (18)F-FLT PET in Relation to Contrast Enhancement in Newly Diagnosed Glioblastoma. J Nucl Med 2021;62(10):1349-1356
https://doi.org/10.2967/jnumed.120.249524

110. Bashir A, Vestergaard MB, Marner L, Larsen VA, Ziebell M, Fugleholm K, Law I. PET imaging of meningioma with 18F-FLT: a predictor of tumour progression. Brain 2020;143(11):3308-3317
https://doi.org/10.1093/brain/awaa267

111. Toyota Y, Miyake K, Kawai N, Hatakeyama T, Yamamoto Y, Toyohara J, et al. Comparison of 4'-[methyl-(11)C]thiothymidine ((11)C-4DST) and 3'-deoxy-3'-[(18)F]fluorothymidine ((18)F-FLT) PET/CT in human brain glioma imaging. EJNMMI Res 2015;5:7
https://doi.org/10.1186/s13550-015-0085-3

112. Nomura N, Pastorino S, Jiang P, Lambert G, Crawford JR, Gymnopoulos M, et al. Prostate specific membrane antigen (PSMA) expression in primary gliomas and breast cancer brain metastases. Cancer Cell Int 2014;14(1):26
https://doi.org/10.1186/1475-2867-14-26

113. Sasikumar A, Joy A, Pillai MR, Nanabala R, Anees KM, Jayaprakash PG, et al. Diagnostic Value of 68Ga PSMA-11 PET/CT Imaging of Brain Tumors-Preliminary Analysis. Clin Nucl Med 2017;42(1):e41-e48
https://doi.org/10.1097/RLU.0000000000001451

114. Salas Fragomeni RA, Pienta KJ, Pomper MG, Gorin MA, Rowe SP. Uptake of Prostate-Specific Membrane Antigen-Targeted 18F-DCFPyL in Cerebral Radionecrosis: Implications for Diagnostic Imaging of High-Grade Gliomas. Clin Nucl Med 2018;43(11):e419-e421
https://doi.org/10.1097/RLU.0000000000002280

115. Kumar A, ArunRaj ST, Bhullar K, Haresh KP, Gupta S, Ballal S, et al. Ga-68 PSMA PET/CT in recurrent high-grade gliomas: evaluating PSMA expression in vivo. Neuroradiology 2022;64(5):969-979
https://doi.org/10.1007/s00234-021-02828-2

116. Matsuda M, Ishikawa E, Yamamoto T, Hatano K, Joraku A, Iizumi Y, et al. Potential use of prostate specific membrane antigen (PSMA) for detecting the tumor neovasculature of brain tumors by PET imaging with (89)Zr-Df-IAB2M anti-PSMA minibody. J Neurooncol 2018;138(3):581-589
https://doi.org/10.1007/s11060-018-2825-5

117. Malric L, Monferran S, Gilhodes J, Boyrie S, Dahan P, Skuli N, et al. Interest of integrins targeting in glioblastoma according to tumor heterogeneity and cancer stem cell paradigm: an update. Oncotarget 2017;8(49):86947-86968
https://doi.org/10.18632/oncotarget.20372

118. Li L, Chen X, Yu J, Yuan S. Preliminary Clinical Application of RGD-Containing Peptides as PET Radiotracers for Imaging Tumors. Front Oncol 2022;12:837952
https://doi.org/10.3389/fonc.2022.837952

119. Schnell O, Krebs B, Carlsen J, Miederer I, Goetz C, Goldbrunner RH, et al. Imaging of integrin alpha(v)beta(3) expression in patients with malignant glioma by [18F] Galacto-RGD positron emission tomography. Neuro Oncol 2009;11(6):861-870
https://doi.org/10.1215/15228517-2009-024

120. Lopci E, Grassi I, Chiti A, Nanni C, Cicoria G, Toschi L, et al. PET radiopharmaceuticals for imaging of tumor hypoxia: a review of the evidence. Am J Nucl Med Mol Imaging 2014;4(4):365-384

121. Mapelli P, Picchio M. 18F-FAZA PET imaging in tumor hypoxia: A focus on high-grade glioma. Int J Biol Markers 2020;35(1_suppl):42-46
https://doi.org/10.1177/1724600820905715

122. Gangemi V, Mignogna C, Guzzi G, Lavano A, Bongarzone S, Cascini GL, et al. Impact of [(64)Cu][Cu(ATSM)] PET/CT in the evaluation of hypoxia in a patient with Glioblastoma: a case report. BMC Cancer 2019;19(1):1197
https://doi.org/10.1186/s12885-019-6368-8

123. Mapelli P, Callea M, Fallanca F, Castellano A, Bailo M, Scifo P, et al. 18F-FAZA PET/CT in pretreatment assessment of hypoxic status in high-grade glioma: correlation with hypoxia immunohistochemical biomarkers. Nucl Med Comm 2021;42(7):763-771
https://doi.org/10.1097/MNM.0000000000001396

124. Bekaert L, Valable S, Lechapt-Zalcman E, Ponte K, Collet S, Constans JM, et al. [18F]-FMISO PET study of hypoxia in gliomas before surgery: correlation with molecular markers of hypoxia and angiogenesis. Eur J Nucl Med Mol Imaging 2017;44(8):1383-1392
https://doi.org/10.1007/s00259-017-3677-5

125. Abdo RA, Lamare F, Fernandez P, Bentourkia M. Analysis of hypoxia in human glioblastoma tumors with dynamic 18F-FMISO PET imaging. Australas Phys Eng Sci Med 2019;42(4):981-993
https://doi.org/10.1007/s13246-019-00797-8

126. Kobayashi K, Manabe O, Hirata K, Yamaguchi S, Kobayashi H, Terasaka S, et al. Influence of the scan time point when assessing hypoxia in (18)F-fluoromisonidazole PET: 2 vs. 4 h. Eur J Nucl Med Mol Imaging 2020;47(8):1833-1842
https://doi.org/10.1007/s00259-019-04626-8

127. Beppu T, Terasaki K, Sasaki T, Fujiwara S, Matsuura H, Ogasawara K, et al. Standardized uptake value in high uptake area on positron emission tomography with 18F-FRP170 as a hypoxic cell tracer correlates with intratumoral oxygen pressure in glioblastoma. Mol Imaging Biol 2014;16(1):127-135
https://doi.org/10.1007/s11307-013-0670-7

128. Toyonaga T, Yamaguchi S, Hirata K, Kobayashi K, Manabe O, Watanabe S, et al. Hypoxic glucose metabolism in glioblastoma as a potential prognostic factor. Eur J Nucl Med Mol Imaging 2017;44(4):611-619
https://doi.org/10.1007/s00259-016-3541-z

129. Gammon ST, Pisaneschi F, Bandi ML, Smith MG, Sun Y, Rao Y, et al. Mechanism-Specific Pharmacodynamics of a Novel Complex-I Inhibitor Quantified by Imaging Reversal of Consumptive Hypoxia with [(18)F]FAZA PET In Vivo. Cells 2019;8(12):1487
https://doi.org/10.3390/cells8121487

130. Barbieri F, Bajetto A, Pattarozzi A, Gatti M, Wurth R, Thellung S, et al. Peptide receptor targeting in cancer: the somatostatin paradigm. Int J Pept 2013;2013:926295
https://doi.org/10.1155/2013/926295

131. Kiviniemi A, Gardberg M, Kivinen K, Posti JP, Vuorinen V, Sipila J, et al. Somatostatin receptor 2A in gliomas: Association with oligodendrogliomas and favourable outcome. Oncotarget 2017;8(30):49123-49132
https://doi.org/10.18632/oncotarget.17097

132. Sommerauer M, Burkhardt JK, Frontzek K, Rushing E, Buck A, Krayenbuehl N, et al. 68Gallium-DOTATATE PET in meningioma: A reliable predictor of tumor growth rate? Neuro Oncol 2016;18(7):1021-1027
https://doi.org/10.1093/neuonc/now001

133. Lapa C, Linsenmann T, Luckerath K, Samnick S, Herrmann K, Stoffer C, et al. Tumor-associated macrophages in glioblastoma multiforme-a suitable target for somatostatin receptor-based imaging and therapy? PloS One 2015;10(3):e0122269
https://doi.org/10.1371/journal.pone.0122269

134. Silva CB, Ongaratti BR, Trott G, Haag T, Ferreira NP, Leaes CG, et al. Expression of somatostatin receptors (SSTR1-SSTR5) in meningiomas and its clinicopathological significance. Int J Clin Exp Pathol 2015;8(10):13185-13192

135. Palmisciano P, Watanabe G, Conching A, Ogasawara C, Ferini G, Bin-Alamer O, et al. The Role of [(68)Ga]Ga-DOTA-SSTR PET Radiotracers in Brain Tumors: A Systematic Review of the Literature and Ongoing Clinical Trials. Cancers 2022;14(12):2925
https://doi.org/10.3390/cancers14122925

136. Vallee E, Paquet N, Buteau JP, Turcotte E. 68Ga-DOTATATE Uptake in Ischemic Stroke. Clin Nucl Med 2018;43(1):46-47
https://doi.org/10.1097/RLU.0000000000001894

137. Zhang J, Li D, Lang L, Zhu Z, Wang L, Wu P, et al. 68Ga-NOTA-Aca-BBN(7-14) PET/CT in Healthy Volunteers and Glioma Patients. J Nucl med 2016;57(1):9-14
https://doi.org/10.2967/jnumed.115.165316

138. Li D, Zhang J, Chi C, Xiao X, Wang J, Lang L, et al. First-in-human study of PET and optical dual-modality image-guided surgery in glioblastoma using (68)Ga-IRDye800CW-BBN. Theranostics 2018;8(9):2508-2520
https://doi.org/10.7150/thno.25599

139. Sun J, Cai L, Zhang K, Zhang A, Pu P, Yang W, et al. A pilot study on EGFR-targeted molecular imaging of PET/CT With 11C-PD153035 in human gliomas. Clin Nucl Med 2014;39(1):e20-26
https://doi.org/10.1097/RLU.0b013e3182a23b73

140. Bova V, Filippone A, Casili G, Lanza M, Campolo M, Capra AP, et al. Adenosine Targeting as a New Strategy to Decrease Glioblastoma Aggressiveness. Cancers 2022;14(16):4032
https://doi.org/10.3390/cancers14164032

141. Bauer A, Langen KJ, Bidmon H, Holschbach MH, Weber S, Olsson RA, et al. 18F-CPFPX PET identifies changes in cerebral A1 adenosine receptor density caused by glioma invasion. J Nucl Med 2005;46(3):450-454

142. Lai TH, Toussaint M, Teodoro R, Dukić-Stefanović S, Gündel D, Ludwig FA, et al. Improved in vivo PET imaging of the adenosine A(2A) receptor in the brain using [(18)F]FLUDA, a deuterated radiotracer with high metabolic stability. Eur J Nucl Med Mol Imaging 2021;48(9):2727-2736
https://doi.org/10.1007/s00259-020-05164-4

143. Postnov A, Toutain J, Pronin I, Valable S, Gourand F, Kalaeva D, et al. First-in-Man Noninvasive Initial Diagnostic Approach of Primary CNS Lymphoma Versus Glioblastoma Using PET With 18 F-Fludarabine and l -[methyl- 11 C]Methionine. Clin Nucl Med 2022;47(8):699-706
https://doi.org/10.1097/RLU.0000000000004238

144. Pannell M, Economopoulos V, Wilson TC, Kersemans V, Isenegger PG, Larkin JR, et al. Imaging of translocator protein upregulation is selective for pro-inflammatory polarized astrocytes and microglia. Glia 2020;68(2):280-297
https://doi.org/10.1002/glia.23716

145. El Chemali L, Akwa Y, Massaad-Massade L. The mitochondrial translocator protein (TSPO): a key multifunctional molecule in the nervous system. Biochem J 2022;479(13):1455-1466
https://doi.org/10.1042/BCJ20220050

146. Ammer LM, Vollmann-Zwerenz A, Ruf V, Wetzel CH, Riemenschneider MJ, Albert NL, et al. The Role of Translocator Protein TSPO in Hallmarks of Glioblastoma. Cancers 2020;12(10):2973
https://doi.org/10.3390/cancers12102973

147. Zinnhardt B, Müther M, Roll W, Backhaus P, Jeibmann A, Foray C, et al. TSPO imaging-guided characterization of the immunosuppressive myeloid tumor microenvironment in patients with malignant glioma. Neuro Oncol 2020;22(7):1030-1043
https://doi.org/10.1093/neuonc/noaa023

148. Su Z, Herholz K, Gerhard A, Roncaroli F, Du Plessis D, Jackson A, et al. [(1)(1)C]-(R)PK11195 tracer kinetics in the brain of glioma patients and a comparison of two referencing approaches. Eur J Nucl Med Mol Imaging 2013;40(9):1406-1419
https://doi.org/10.1007/s00259-013-2447-2

149. Roncaroli F, Su Z, Herholz K, Gerhard A, Turkheimer FE. TSPO expression in brain tumours: is TSPO a target for brain tumour imaging? Clin Transl Imaging 2016;4:145-156
https://doi.org/10.1007/s40336-016-0168-9

150. Tan MH, Li J, Xu HE, Melcher K, Yong EL. Androgen receptor: structure, role in prostate cancer and drug discovery. Acta Pharmacol Sin 2015;36(1):3-23
https://doi.org/10.1038/aps.2014.18

151. Zhao N, Wang F, Ahmed S, Liu K, Zhang C, Cathcart SJ, et al. Androgen Receptor, Although Not a Specific Marker For, Is a Novel Target to Suppress Glioma Stem Cells as a Therapeutic Strategy for Glioblastoma. Front Oncol 2021;11:616625
https://doi.org/10.3389/fonc.2021.616625

152. Orevi M, Shamni O, Zalcman N, Chicheportiche A, Mordechai A, Moscovici S, et al. [(18)F]-FDHT PET/CT as a tool for imaging androgen receptor expression in high-grade glioma. Neurooncol Adv 2021;3(1):vdab019
https://doi.org/10.1093/noajnl/vdab019

153. Hall LT, Titz B, Robins HI, Bednarz BP, Perlman SB, Weichert JP, et al. PET/CT imaging of the diapeutic alkylphosphocholine analog (124)I-CLR1404 in high and low-grade brain tumors. Am J Nucl Med Mol Imaging 2017;7(4):157-166

154. Clark PA, Al-Ahmad AJ, Qian T, Zhang RR, Wilson HK, Weichert JP, et al. Analysis of Cancer-Targeting Alkylphosphocholine Analogue Permeability Characteristics Using a Human Induced Pluripotent Stem Cell Blood-Brain Barrier Model. Mol Pharm 2016;13(9):3341-3349 https://doi.org/10.1021/acs.molpharmaceut.6b00441

155. Hall LT, Titz B, Baidya N, van der Kolk AG, Robins HI, Otto M, et al. [(124)I]CLR1404 PET/CT in High-Grade Primary and Metastatic Brain Tumors. Mol Imaging Biol 2020;22(2):434-443 https://doi.org/10.1007/s11307-019-01362-1

156. Oborski MJL, Lieberman FS, Qian Y, Drappatz J, Mountz JM. [18F]ML-10 PET: Initial Experience in Glioblastoma Multiforme Therapy Response Assessment. Tomography 2016;2(4):8 https://doi.org/10.18383/j.tom.2016.00175

157. Panichelli P, Villano C, Cistaro A, Bruno A, Barbato F, Piccardo A, et al. Imaging of Brain Tumors with Copper-64 Chloride: Early Experience and Results. Cancer Biother Radiopharm 2016;31(5):159-167 https://doi.org/10.1089/cbr.2016.2028

158. Maugeri R, Schiera G, Di Liegro CM, Fricano A, Iacopino DG, Di Liegro I. Aquaporins and Brain Tumors. Int J Mol Sci 2016;17(7):1029 https://doi.org/10.3390/ijms17071029

159. Suzuki Y, Nakamura Y, Yamada K, Kurabe S, Okamoto K, Aoki H, et al. Aquaporin Positron Emission Tomography Differentiates Between Grade III and IV Human Astrocytoma. Neurosurg 2018;82(6):842-846 https://doi.org/10.1093/neuros/nyx314

160. Behr SC, Villanueva-Meyer JE, Li Y, Wang YH, Wei J, Moroz A, et al. Targeting iron metabolism in high-grade glioma with 68Ga-citrate PET/MR. JCI Insight 2018;3(21):e93999 https://doi.org/10.1172/jci.insight.93999

161. Shen Y, Li X, Dong D, Zhang B, Xue Y, Shang P. Transferrin receptor 1 in cancer: a new sight for cancer therapy. Am J Cancer Res 2018;8(6):916-931

162. Fitzgerald AA, Weiner LM. The role of fibroblast activation protein in health and malignancy. Cancer Metastasis Rev 2020;39(3):783-803 https://doi.org/10.1007/s10555-020-09909-3

163. Mori Y, Dendl K, Cardinale J, Kratochwil C, Giesel FL, Haberkorn U. FAPI PET: Fibroblast Activation Protein Inhibitor Use in Oncologic and Nononcologic Disease. Radiology 2023;306(2):e220749 https://doi.org/10.1148/radiol.220749

164. Yao Y, Tan X, Yin W, Kou Y, Wang X, Jiang X, et al. Performance of (18) F-FAPI PET/CT in assessing glioblastoma before radiotherapy: a pilot study. BMC Med Imaging 2022;22(1):226 https://doi.org/10.1186/s12880-022-00952-w

165. Gilardi L, Airò Farulla LS, Demirci E, Clerici I, Omodeo Salè E, Ceci F. Imaging Cancer-Associated Fibroblasts (CAFs) with FAPi PET. Biomedicines 2022;10(3):523 https://doi.org/10.3390/biomedicines10030523

166. Röhrich M, Loktev A, Wefers AK, Altmann A, Paech D, Adeberg S, et al. IDH-wildtype glioblastomas and grade III/IV IDH-mutant gliomas show elevated tracer uptake in fibroblast activation protein-specific PET/CT. Eur J Nucl Med Mol Imaging 2019;46(12):2569-2580
https://doi.org/10.1007/s00259-019-04444-y

167. Shi Y, Riese DJ, 2nd, Shen J. The Role of the CXCL12/CXCR4/CXCR7 Chemokine Axis in Cancer. Front Pharm 2020;11:574667
https://doi.org/10.3389/fphar.2020.574667

168. Zhao H, Guo L, Zhao H, Zhao J, Weng H, Zhao B. CXCR4 over-expression and survival in cancer: a system review and meta-analysis. Oncotarget 2015;6(7):5022-5040
https://doi.org/10.18632/oncotarget.3217

169. Lapa C, Lückerath K, Kleinlein I, Monoranu CM, Linsenmann T, Kessler AF, et al. (68)Ga-Pentixafor-PET/CT for Imaging of Chemokine Receptor 4 Expression in Glioblastoma. Theranostics 2016;6(3):428-434
https://doi.org/10.7150/thno.13986

170. Chen Z, Yang A, Zhang J, Chen A, Zhang Y, Huang C, et al. CXCR4-Directed PET/CT with [(68)Ga]Pentixafor in Central Nervous System Lymphoma: A Comparison with [(18)F]FDG PET/CT. Mol Imaging Biol 2022;24(3):416-424
https://doi.org/10.1007/s11307-021-01664-3

171. Jacobs SM, Wesseling P, de Keizer B, Tolboom N, Ververs FFT, Krijger GC, et al. CXCR4 expression in glioblastoma tissue and the potential for PET imaging and treatment with [(68)Ga]Ga-Pentixafor /[(177)Lu]Lu-Pentixather. Eur J Nucl Med Mol Imaging 2022;49(2):481-491
https://doi.org/10.1007/s00259-021-05196-4

172. Rotoli D, Cejas MM, Maeso MD, Pérez-Rodríguez ND, Morales M, Ávila J, et al. The Na, K-ATPase β-Subunit Isoforms Expression in Glioblastoma Multiforme: Moonlighting Roles. Int J Mol Sci 2017;18(11):2369
https://doi.org/10.3390/ijms18112369

173. Parent EE, Sethi I, Nye J, Holder C, Olson JJ, Switchenko J, et al. 82Rubidium chloride positron emission tomography discrimination of recurrent intracranial malignancy from radiation necrosis. Q J Nucl Med Mol Imaging 2022;66(1):74-81
https://doi.org/10.23736/S1824-4785.19.03173-X

174. Kostenikov NA, Zhuikov BL, Chudakov VM, Iliuschenko YR, Shatik SV, Zaitsev VV, et al. Application of (82) Sr/(82) Rb generator in neurooncology. Brain Behav 2019;9(3):e01212
https://doi.org/10.1002/brb3.1212

175. Cheng X, Zhu W, Cui R. Increased 18F-2-Fluorodeoxysorbitol (18F-FDS) Activity in a Pituitary Spindle Cell Carcinoma. Clin Nucl Med 2016;41(12):953-955
https://doi.org/10.1097/RLU.0000000000001391

176. Song IU, Lee SH, Chung YA. The incidental suggestive meningioma presenting as high 18F FP-CIT uptake on PET/CT study. Clin Nucl Med 2014;39(1):e97-98
https://doi.org/10.1097/RLU.0b013e3182815d16

177. Doi S, Kashiwagi N, Satou T, Kaida H, Ishi K. Pittsburgh Compound-B Uptake in Meningioma With Histopathologic Correlation. Clin Nucl Med 2019;44(7):587-588
https://doi.org/10.1097/RLU.0000000000002590

178. Albert NL, Weller M, Suchorska B, Galldiks N, Soffietti R, Kim MM, et al. Response Assessment in Neuro-Oncology working group and European Association for Neuro-Oncology recommendations for the clinical use of PET imaging in gliomas. Neuro Oncol 2016;18(9):1199-1208
https://doi.org/10.1093/neuonc/now058

Table 1 Concise overview of clinical trial results of PET agents for brain tumor imaging

PET agent	Highlights in imaging	Uptake vs. molecular markers	Limitations	Trials*	Figure
Nutrient-based agents					
^{18}F-FDG	Improves tumor grade differentiation Identifies malignant transformation in LGG Particularly useful in evaluating lymphomas	Pos. correlation with MGMT methylation	Significant background uptake Low specificity (e.g. inflammation)	NCT02391246 NCT01801371 NCT02327442 NCT04407039 NCT03732352 NCT03583528 NCT04566185 NCT02125786 NCT02902757 NCT04315584	2, 3
^{18}F-Me-4FDG	High uptake in HGG	Unknown	Role BBB permeability unclear	-	2, 3
^{11}C-MET	Improves tumor delineation Improves tumor type differentiation Increased uptake → worse prognosis	Pos. correlation with: - Tumor cell density - MGMT promotor methylation - 1p19q co-deletion Neg. correlation with IDH mutation	Less successful in grade differentiation Low specificity (e.g. inflammation) Short half-life (^{11}C)	NCT02585219 NCT04111588 NCT04065776 NCT03739333 NCT05608395 NCT00840047 NCT05589961 NCT04391062 NCT02125786 NCT03732352 NCT03583528 NCT04566185 NCT02125786 NCT02902757 NCT04315584	2, 4
^{11}C-TYR	Uptake in variety of brain tumors	No correlation with Ki-67	Questionable whether really reflecting protein synthesis & cell progression Short half-life (^{11}C)	-	2
^{11}C-MCYS	High uptake in recurrent glioblastoma	Unknown	Significant background uptake Short half-life (^{11}C)	-	2

^{18}F-FDOPA	Higher sensitivity than ^{18}F-FDG Improves LGG-HGG differentiation Increased uptake → worse prognosis	Pos. correlation with Ki-67 Pos. correlation with IDH mutation	Variable success in individual tumor grade differentiation Conflicting results in recurrent tumors Physiologic uptake in striatum limits tumor delineation in this area	NCT05512403 NCT04766632 NCT02104310 NCT02020720 NCT01991977 NCT04870580 NCT03778294 NCT01165632 NCT03903419 NCT03932981 NCT05781321 NCT05653622 NCT04315584 NCT04566185	2
^{18}F-FAMT	Higher T/N ratio than ^{18}F-FDG Improves LGG-HGG differentiation	No correlation with Ki-67	Added value over other amino acid PET agents unknown	-	2
^{18}F-FIMP	Higher accumulation in higher-grade gliomas Possibly better retention in cytoplasm Clear images compared to ^{11}C-MET & ^{18}F-FDG	Unknown	Assimilation mechanisms not entirely clear	-	2
^{18}F-FET	Correctly identifies more malignant areas High uptake in recurrent glioblastoma improves tumor delineation	Unknown	Moderate background uptake Less successful in grade differentiation	NCT04111588 NCT04044937 NCT05386043	2, 6
^{18}F-OMFD	Uptake in variety of brain tumors Improves tumor delineation	Unknown	Unknown	-	2
^{18}F-FGln	Uptake in high-grade astrocytomas only High specificity (no uptake in inflammation)	Unknown	Unknown	-	2
^{11}C-ACBC	Higher sensitivity than ^{18}F-FDG	Unknown	Unsuccessful in grade differentiation	-	2
^{18}F-FACBC	Affinity for most malignant tumor areas Lower background uptake than ^{11}C-MET Improves LGG-HGG differentiation	Pos. correlation with Ki-67	Unknown	NCT04111588	2, 4
^{18}F-FSPG	High uptake in recurrent glioma Differences in uptake curves of good vs poor outcomes in oligodendroglioma	Unknown	Role BBB permeability unclear	NCT02370563	2
D-cis-^{18}F-FPro	Uptake associated with cell death	Unknown	Uptake mechanism unclear Role BBB permeability unclear	-	2
^{11}C-MeAIB	Higher T/N ratio than ^{11}C-MET Differentiates low- from high-grade gliomas	Pos. correlation with proliferation markers in cell lines	Role BBB permeability unclear	-	2

^{11}C-AMT	Uptake in LGG and HGG Improves tumor type differentiation Uptake predicts survival Improves tumor delineation Shows uptake in DNET (unique)	Pos. correlation with IDO (LGG) Pos. correlation with LAT1 (HGG)	Image interpretation depends on kinetic analyses (dynamic PET imaging)	-	2
^{18}F-FBPA	Feasibility assessment of BNCT in glioma & meningioma Increased uptake → worse prognosis	Unknown	Additional value over ^{18}F-FDG unclear	-	2
^{18}F-FBY	Solely indicative for LAT1 overexpression due to fast excretion Can be used for treatment (^{19}F-FBY)	Unknown	Unknown	-	2
^{11}C-choline	Fast imaging due to rapid clearance Very low background uptake Uptake in variety of brain tumors	Pos. correlation with Ki-67	Conflicting results regarding LGG-HGG differentiation Low specificity (e.g. inflammation)	NCT01165632	2
^{18}F-FCHO	Fast imaging due to rapid clearance Very low background uptake Uptake meningioma > glioblastoma Uptake grade II-III glioma highly variable	Unknown	Low specificity (e.g. inflammation)	-	2
^{11}C-acetate	Improves grade IV vs. lower grade differentiation	Unknown	Unknown	-	2
^{13}N-ammonia	Improves LGG-HGG differentiation Sensitivity in LGG → astrocytoma component	Unknown	Unsuccessful in individual tumor grade differentiation Unclear if uptake reflects ↑ metabolism or BBB breakdown	-	2
^{18}F-DASA-23	High T/N ratio PKM2 also therapeutic target	Unknown	Unclear transport mechanism	NCT03539731	2
Nucleoside-based agents					
^{11}C-TdR	Improves tumor grade differentiation	Unknown	High background uptake due to BBB-penetrating radioactive metabolites	-	5
^{18}F-FMAU	Little brain parenchymal uptake Improves visualization of recurrent glioma	Unknown	Unknown	NCT04752267	5
^{18}F-FLT	High sensitivity for HGG Heterogeneous uptake in LGG Improves HGG differentiation	Pos. correlation with Ki-67 (even more than ^{11}C-MET)	Significant role transport through BBB Less successful in LGG differentiation	NCT04309552	5, 6
^{11}C-4DST	High sensitivity for HGG Improves tumor grade differentiation	Pos. correlation with Ki-67	LGG detection worse than ^{11}C-MET High background uptake suggests radioactive metabolites	-	5

Receptor-based agents					
^{68}Ga-PSMA	High uptake in HGG Improves tumor recurrence detection	Unknown	Role BBB permeability unclear	NCT05798273 NCT05644080 NCT03903419	7
^{18}F-DCFPyL	Binds PSMA in glioblastoma microvessels Binds PSMA on grade III astrocytoma cells	Unknown	Role BBB permeability unclear	-	7
^{89}Zr-Df-IAB2M	High sensitivity for HGG & grade I astrocytoma	Trend for correlation with PSMA	Unknown	-	7
^{18}F-galacto-RGD	Heterogeneous uptake within tumor	Pos. correlation with Integrin $\alpha_v\beta_3$	Possibly low affinity for Integrin $\alpha_v\beta_3$	NCT01939574	7
^{18}F-FPPRGD2	Improves tumor delineation Improves LGG-HGG differentiation	Unknown	Unknown	NCT02441972	7
^{18}F-RGD	Uptake predicts treatment sensitivity	Unknown	Unknown	-	7
^{68}Ga-PRGD2	Higher T/N ratio than ^{18}F-FDG	Unknown	Unknown	NCT01801371 NCT02666547	7
^{68}Ga-DOTATATE	High uptake in meningiomas Improves tumor delineation Higher sensitivity vs. contrast-enhanced MRI Increased uptake → faster growth	Pos. correlation with SSTR2	Unknown	NCT04081701	7
^{68}Ga-DOTATOC	High uptake in meningiomas Improves tumor delineation Higher sensitivity vs. contrast-enhanced MRI Increased uptake → faster growth	Pos. correlation with SSTR2	Uptake HGG correlated with BBB permeability instead of SSTR2 expression	NCT03583528	7
^{68}Ga-DOTANOC	Increased uptake in HGG	Unknown	Uptake HGG correlated with BBB permeability instead of SSTR2 expression	-	7
^{68}Ga-BBN	Focus on patient stratification for secondary treatment with GRPR-targeted agents Prominent uptake in contrast-enhancing tumors irrespective of WHO grade	Pos. correlation with GRPR	Role BBB permeability unclear	NCT03407781 NCT02910804	7
^{11}C-PD153035	Focus on patient stratification for secondary treatment with EGFR-targeted agents	Pos. correlation with EGFR	Unknown	-	7
^{18}F-CPFPX	Increased uptake in tissue surrounding glioblastoma	Unknown	Elusive function A_1AR in oncogenesis Role of BBB permeability unclear	-	7
^{18}F-FLUDA	May be able to differentiate primary CNS lymphoma from glioblastoma	Unknown	Role of BBB permeability unclear	-	7
^{11}C-PK11195	Improves LGG-HGG differentiation	Unknown	Unclear role of TSPO in oncogenesis	-	7

^{18}F-DPA-714	Visualizes inflammatory cells within the tumor microenvironment	Pos. correlation with no. of glioma-associated myeloid cells	Unclear role of TSPO in oncogenesis	NCT05672082 NCT04171882 NCT05128903	7
^{18}F-FDHT	Very low background uptake	Unknown	Role BBB permeability unclear Uptake intensity relatively low	-	7
^{11}C-TGN-020	High uptake grade III-IV astrocytoma Improves tumor grade differentiation	Pos. correlation with AQP1 and -4	Unknown	-	7, 9
^{68}Ga-citrate	Very low background uptake	Unknown	Unknown	-	7
^{68}Ga(-DOTA)-FAPI	Low background activity Improves LGG-HGG differentiation	Unknown	Role of BBB permeability unclear	NCT04554719 NCT04459273	7
^{18}F-FAPI	Long background activity	Unknown	Role of BBB permeability unclear	-	7
^{68}Ga-Pentixafor	High uptake in CNS lymphoma and glioblastoma Therapeutic potential (^{177}Lu/^{90}Y)	Conflicting results	Role of BBB permeability unclear Inconsistent correlation between uptake and CXCR4 expression	-	7
TME-based and miscellaneous agents					
^{18}F-EF5	Heterogeneous uptake in glioblastoma Uptake corresponds to areas of hypoxia	Unknown	Relatively difficult to synthesize	-	8
^{62}Cu^{2+}-ATSM	Improves grade IV vs. lower grade differentiation Specific sensitivity to astrocytoma component	Pos. correlation with HIF-1	Agent might not reflect hypoxia but another metabolic upregulation	-	8
^{18}F-FAZA	Faster clearance vs. ^{18}F-FMISO Improved T/N ratios vs. ^{18}F-FMISO Very high uptake in high-grade gliomas	Pos. correlation with VEGF No correlation with HIF-1	Influence of BBB permeability unclear	NCT05047913	8
^{18}F-FRP170	High uptake in HGG (between necrotic center and outer contrast-enhancing tumor layer)	Pos. correlation with HIF-1 No correlation with Ki-67	Unknown	-	8
^{18}F-FMISO	High uptake in glioblastoma Improved tumor grade differentiation Uptake predicts survival	(Variable) Pos. correlation with: - HIF-1 - VEGF	Less consistent uptake in grade II-III gliomas Slow target tissue accumulation & clearance of healthy tissue	NCT04309552 NCT05500612	8
^{124}I-CLR1404	High T/N ratio in recurrent astrocytoma	Unknown	Unknown	-	8
^{18}F-ML-10	Focus on treatment assessment Changes in uptake pattern during treatment	Unknown	No correlation with progression Relatively low specificity Difficulties in image interpretation due to tumor heterogeneity	-	8

$^{64}CuCl_2$	High uptake in glioblastomas No uptake in grade II astrocytomas	Unknown	Unclear whether it can cross BBB Role Ctr1 in oncogenesis not completely elucidated	-	8
^{82}Rb-Chloride	Differentiates between low- and high-grade tumors	Unknown	Relatively nonspecific agent Role of BBB permeability unclear	-	8
^{18}F-FDS	High uptake spindle cell carcinoma pituitary	Unknown	Role BBB permeability unclear	-	N/A
^{18}F-FP-CIT	Improves meningioma vs. other tumor type differentiation	Unknown	Contradictory results on presence of β-amyloid within meningioma	-	N/A
^{11}C-PiB	High uptake in meningioma	Unknown	Role DAT in oncogenesis unknown	-	N/A

* Active trials using the specific PET agent for brain tumor imaging, as reported on www.clinicaltrials.gov

Abbreviations: A_1AR, A_1 adenosine receptor; AQP, aquaporin; BBB, blood-brain barrier; BNCT, boron neutron capture therapy; Ctr1, copper transporter 1; DAT, dopamine active transporter; DNET, dysembryoplastic neuroepithelial tumor; EGFR, epidermal growth factor receptor; GRPR, gastrin releasing peptide receptor; HGG, high-grade glioma; HIF, hypoxia-inducible factors; IDH, isocitrate dehydrogenase; IDO, indoleamine 2,3-dioxygenase; Ki-67, cellular proliferation activity index; LAT, large neutral amino acid transporter; LGG, low-grade glioma; MGMT, O^6-methylguanine-DNA-methyltransferase; MRI, magnetic resonance imaging; N/A, not applicable; PET, positron emission tomography; PSMA, prostate-specific membrane antigen; SSTR, somatostatin receptor; SUV, standardized uptake value; TME, tumor microenvironment; T/N ratio, tumor-to-normal-tissue ratio; TSPO, translocator protein; VEGF, vascular endothelial growth factor; WHO, World Health Organization.

Table 2 Occurrence and effects of common (genetic) changes in brain tumors; see also ***Figure 1***

(Genetic) change	Effect	Additional info	Brain tumor type*
PTEN mutation / deletion	**Increased energy metabolism & angiogenesis** by stimulating PI3K-AKT-mTORC signaling pathway	PI3K-AKT-mTORC signaling pathway also stimulated by ↑ tumoral secretion of growth factors (PDGF, EGF, TNF-α)	Glioblastoma, IDH-wildtype Glioblastoma, IDH-mutant (minimal)
TP53 mutation (most common) / inactivation of p53 protein	**Increased energy metabolism & angiogenesis** by stimulating PI3K-AKT-mTORC signaling pathway DNA damage repair dysregulation, **cell cycle progression** and apoptosis	Occurs in virtually all tumor types	Astrocytoma grade II, III Oligodendroglioma grade II, III Pleomorphic xanthoastrocytoma grade II, III (minimal) Glioblastoma, IDH-wildtype Glioblastoma, IDH-mutant
EGFR mutation / amplification	**Increased energy metabolism & angiogenesis** by upregulating PI3K-AKT-mTORC signaling pathway through increased signaling of EGFR	PI3K-AKT-mTORC signaling pathway also stimulated by ↑ tumoral secretion of growth factors (PDGF, EGF, TNF-α)	Glioblastoma, IDH-wildtype Glioblastoma, IDH-mutant (minimal)
NF1 mutation	**Cell cycle progression** by activating Ras independent of growth factors	Ras-Raf-MEK-ERK(MAPK) signaling pathway also stimulated by ↑ tumoral secretion of growth factors (PDGF, EGF, TNF-α)	Glioblastoma, IDH-wildtype
BRAF mutation	**Cell cycle progression** by activating Raf independent of growth factors	Ras-Raf-MEK-ERK(MAPK) signaling pathway also stimulated by ↑ tumoral secretion of growth factors (PDGF, EGF, TNF-α)	Pilocytic astrocytoma Pleomorphic xanthoastrocytoma grade II, III Craniopharyngioma Glioblastoma, IDH-wildtype (minimal)
COX2 overexpression	Stimulates Ras-Raf-MEK-ERK(MAPK) signaling pathway through EGFR	-	Astrocytoma grade II, III Glioblastoma, IDH-wildtype (?) Glioblastoma, IDH-mutant (?)
MYC overexpression	Stimulates many molecular pathways by increased gene transcription Regulates and stimulates proliferation of highly malignant tumor cell subtype (tumor stem-like cell)	MYC protein functions as general transcription factor for variety of genes associated with normal development; sustained- or over-expression found in virtually all tumor types & seen as major driving force in oncogenesis	Medulloblastoma Glioblastoma, IDH-mutant Glioblastoma, IDH-wildtype (?)
INK4/ARF (tumor suppressor locus) mutation / deletion	Inactivates p53 protein by reduced ARF synthesis Inactivates Rb1 protein by reduced INK4a and INK4b synthesis	ARF normally inhibits MDM2 from impeding p53 function INK4a and INK4b normally inhibit CDK4/6 and Cyclin D activity	Astrocytoma grade II, III (less) Pleomorphic xanthoastrocytoma grade II, III Glioblastoma, IDH-wildtype
MDM2 / MDM4 gene overexpression	Inhibits activity of p53 protein & stimulates its degradation	-	Glioblastoma, IDH-mutant (minimal) Glioblastoma, IDH-wildtype
Rb1 mutation / ↑ expression Rb1 regulators Cyclin D, CDK4 & CDK6 (more common)	**Cell cycle progression** by Increases gene transcription	Rb1 (tumor suppressor protein) normally inhibits CDKs, stabilizes chromosome structure & binds E2F transcription factors → inhibits gene transcription & subsequent cell cycle	Glioblastoma, IDH-wildtype

		progression; Cyclin D, CDK4 and CDK6 cause detachment of E2F from Rb.	
MGMT promoter methylation	**Decreased DNA repair** due to ↓ DNA repair protein MGMT because of impossible gene transcription	'Positive' methylation status → oncogenic genetic alterations will survive, but DNA damage caused by chemotherapeutical agents will also evade repair → chemotherapy-induced	Astrocytoma grade II, III Oligodendroglioma grade II, III Glioblastoma, IDH-wildtype Glioblastoma, IDH-mutant
IDH1/2 (neomorph) mutation	**Increased energy metabolism & angiogenesis** by mTORC activation (and blocking of cellular differentiation) due to ↑ production of (accumulating) 2HG	Mutations result in IDH protein with new function, converting α-KG to 2HG; tumor cell will compensate for altered flux of α-KG by increasing glutaminolysis; IDH-mutated tumors often associated with younger age at diagnosis & better prognosis	Astrocytoma grade II, III Oligodendroglioma grade II, III Glioblastoma, IDH-mutant
ATRX mutation	↑ **cellular survival** & telomere conservation by upregulating ATRX causing ↑ alternative lengthening of telomeres	Often seen together with IDH mutations; amount of cell divisions normally limited by length of telomeres, where successive cell divisions shorten telomeres, leading to cellular 'ageing' and death.	Astrocytoma grade II, III Glioblastoma, IDH-mutant
TERT mutation	↑ **cellular survival** & telomere conservation by upregulating TERT causing ↑ telomerase activity	Often seen together with IDH mutations; amount of cell divisions normally limited by length of telomeres, where successive cell divisions shorten telomeres, leading to cellular 'ageing' and death.	Meningioma Oligodendroglioma grade II, III Medulloblastoma Glioblastoma, IDH-wildtype Glioblastoma, IDH-mutant (less)
1p19q co-deletion	Unknown	Key molecular feature of oligodendroglioma in 2016 WHO classification of brain tumors	Oligodendroglioma grade II, III

* Based on the WHO 2016 classification, considering most studies discussed in this book chapter were published before the 2021 WHO update.

Abbreviations: 2HG, 2-hydroxyglutarate; α-KG, alpha-ketoglutarate; AKT, protein kinase B; ARF, ADP ribosylation factor; ATRX, alpha thalassemia / mental retardation syndrome X-linked; CDK, cyclin-dependent kinase; COX, cyclooxygenase; DNA, deoxyribonucleic acid; EGF, epidermal growth factor and EGFR, its receptor; ERK, extracellular signal-regulated kinases; IDH, isocitrate dehydrogenase; MAPK, mitogen-activated protein kinase; MDM, E3 ubiquitin-protein ligase; MGMT, O^6-methylguanine-DNA-methyltransferase; mTORC, mechanistic target of rapamycin complex 1; NF, neurofibromatosis; PDGF, platelet-derived growth factor; PI3K, phosphatidylinositol 3-kinase; PTEN, phosphatase and tensin

homolog; Rb, retinoblastoma protein; TERT, telomerase reverse transcriptase; TNF-α, tumor necrosis factor alpha; WHO, world health organization.

Table 3 Tissue expression of transporters and receptors used by brain tumor PET agents in humans (alphabetically)

Transporter / Receptor	Associated PET agent(s)	Expression in healthy brain*	Expression in brain tumors*	Remarks
A_1AR	^{18}F-CPFPX	Microglia/macrophages Neurons Other immune cells	Unknown	Plays crucial role in activation of expressed cells
$A_{2A}AR$	^{18}F-FLUDA	Neurons (pre- and postsynaptic) Astrocytes Oligodendrocytes Immune cells (regT cells, macrophages, natural killer cells)	B-lymphocytes, primary CNS lymphoma	May be able to differentiate primary CNS lymphoma from glioblastoma
AR	^{18}F-FDHT	Minimal to none	Tumor cells, nuclei Peri-arterially	Suppresses MYC expression, suggesting role in tumor cell maintenance and proliferation
AQP1/4	^{11}C-TGN-020	Astrocytes (PM; localized to endfeet next to BBB) Neurons Dural and vascular membranes (choroid plezus, ventricular ependymal layer, etc.)	Tumor cells (PM), gliomas & lymphomas Endothelial cells (C + PM), lymphomas	AQP4 in tumors redistributed across complete PM; expression grade I & III gliomas and glioblastoma >> grade II gliomas; highest in peritumoral zone; in lymphomas associated with Ki-67
ASCT2	^{11}C-MCYS, ^{18}F-FGln, ^{11}C-MET, ^{11}C-ACBC, ^{18}F-FACBC	Unknown	Upregulated and activated in gliomas	Increased ^{18}F-FACBC uptake in gliomas due to upregulation and activation of LAT and ASCT
B^0 / B^{0+}	^{18}F-FET	Unknown	Unknown	Uptake through this transporter depends on specific cell type & differences in intra- and extracellular amino acid concentrations
CHT1 - CTL1/3	^{18}F-FCHO, ^{11}C-CHO	Some neurons (PM; grey matter) Endothelial cells (CTL)	N/A	Increased choline (and ^{18}F-FCHO / ^{11}C-CHO) uptake in tumor cell possibly result of increased influx only, instead of overexpression transporter
Ctr1	$^{64}CuCl_2$	Unknown	Unknown	Increased copper (and $^{64}CuCl_2$) uptake in tumor cell possibly result of increased influx only, instead of overexpression transporter
CXCR4	^{68}Ga-Pentixafor	All major CNS cell types, including neurons (but low expression)	Tumor cells, cytoplasm Tumor cells, nuclei Endothelial cells	Large inter- and intra-tumoral variability in expression in glioblastomas
DAT	^{18}F-FP-CIT	Basal ganglia	Unknown	-

EGFR	^{11}C-PD153035	Ependymal cells Some neurons (e.g. hippocampus)	Expression in all glioma subtypes (approx. 50% or tumors per type)	-
ENT-1	^{11}C-TdR, ^{11}C-4DST, ^{18}F-FMAU, ^{18}F-FLT	Unknown	Unknown	Increased nucleoside (and nucleoside-based agent) uptake in tumor cell possibly result of increased influx only, instead of increased transporter
FAP	^{68}Ga(-DOTA)-FAPI, ^{18}F-FAPI	No/little expression on either parenchymal or endothelial cells	Tumor cells, gliomas (?) Tumor microenvironment, near blood vessels, gliomas	While specific for fibroblasts in tumoral stroma of extracranial cancer, in the brain it will likely be present on other cells
GLUT	^{18}F-FDG	Throughout brain (mainly grey matter) including BBB	Unknown	FDG is transported across the intact BBB by GLUT, mainly GLUT1 and GLUT3, which are upregulated in many tumors, especially aggressive tumors
GRPR	^{68}Ga-BBN	Neurons	Endothelial cells, gliomas Tumor cells, gliomas	-
Integrin $\alpha_v\beta_3$	^{18}F-RGD, ^{18}F-galacto-RGD, ^{68}Ga-PRGD2, ^{18}F-FPPRGD2	No/little expression on either parenchymal or endothelial cells	Endothelial cells (PM), gliomas Tumor cells (C + PM, gliomas	Expression glioblastoma > grade II & III glioma & associated with IDH-mutation Expression on activated macrophages, potentially within tumor microenvironment
LAT1	^{18}F-FDOPA, ^{18}F-FET, ^{18}F-FAMT, ^{11}C-MCYS, ^{18}F-FGln, ^{11}C-TYR, ^{11}C-MET, ^{11}C-AMT, ^{11}C-ACBC, ^{18}F-FACBC, ^{18}F-OMFD, ^{18}F-FBPA, ^{18}F-FBY, ^{18}F-FIMP	Endothelial cells	Endothelial cells (C + PM), gliomas Tumor cells (C + PM), gliomas	Highest expression in peritumoral zone; positive correlation between expression & both tumor grade and Ki-67
Na/K-ATPase	^{82}Rb-Chloride	Ubiquitous in all human cells	All tumor-associated cells	Relatively nonspecific enzyme/ion pump, overexpressed in glioblastomas and other brain tumors
PKM2^{+}	^{18}F-DASA-23	No/little expression on either parenchymal or healthy endothelial cells (BBB)	Overexpressed but unknown which specific cells	PKM2 expression is linked to increased glucose uptake, enhanced lactate production & decreased O_2 consumption, and promotes macromolecule synthesis, cell proliferation & growth
PROT	D-cys-^{18}F-Fpro	Unknown	Unknown	-
PSMA	^{18}F-DCFPyL, ^{68}Ga-PSMA, ^{89}Zr-Df-IAB2M	No/little expression on either parenchymal or endothelial cells	Endothelial cells, glioblastoma > grade I astrocytomas Tumor cells (minimal), grade II & III astrocytoma	Virtually no expression in lymphoma
SGLT2	^{19}F-Me-4FDG	No/little expression on either parenchymal or healthy endothelial cells (BBB)	Endothelial cells, glioma Tumor cells (PM), glioma Microglial cells, glioma	Also expression in reactive astrocytes and neurons

SMCT1/2 - MCT1/4	^{11}C-acetate	Endothelial cells (MCT)	Unknown	Increased acetate (and ^{11}C-acetate) uptake in tumor cell possibly result of increased influx only, instead of increased transporter
SSTR1-5	^{68}Ga-DOTATATE, ^{68}Ga-DOTATOC, ^{68}Ga-DOTANOC	Throughout brain	Endothelial cells, meningiomas Tumor cells (C), meningiomas Tumor cells (C + PM), gliomas	Receptor activation has *anti*neoplastic effect so tumor expression puzzling; oligodendrogliomas > IDH-wildtype & -mutant astrocytomas >> glioblastoma; less known about SSTR1 and SSTR3-5 except abundance on meningiomas
System x_c^-	^{18}F-FSPG	No/little expression on either parenchymal or endothelial cells	Tumor cells (C + PM), gliomas	Increased expression in high-grade tumors; inverse correlation between uptake and IDH-mutation
System A	^{11}C-MeAIB	Abluminal membrane of BBB	Unknown	Overexpression related to proliferation grade; associated with malignant transformation
TSPO	^{11}C-PK11195, ^{18}F-DPA-714	Mainly expressed on microglial and ependymal cells; no/little expression on either parenchymal or endothelial cells	Normal endothelial cells in tumor, glioma Tumor cells (C), glioma Tumor-associated macrophages, glioma	Expression is positively correlated with WHO grade and Ki-67 index Increased expression in macrophages, microglia and astrocytes in inflammation

Note: Transporter expression on healthy brain endothelial cells will facilitate BBB permeability of associated PET agent, which has both an advantage and a disadvantage: the PET agent will be able to reach tumor cells even in case of intact BBB, but will also easily reach the healthy brain parenchyma, causing a standard amount of background uptake.

* 'Unknown' means no human immunohistochemical studies have been found for the specific transporter / receptor.

† Not a transporter / receptor but an isoform of the enzyme pyruvate kinase

Abbreviations: A_1AR, adenosine A1 receptor; A_{2A}AR, adenosine A_{2A} receptor; AQP1/4, aquaporin-1/4; AR, androgen receptor; ASCT, anti-neutral amino acid transporter; BBB, blood-brain barrier; C, cytoplasm; CHT1, high-affinity choline transporter-1; CTL1, choline transporter-like protein-1; Ctr1, copper transporter-1; CXCR4, C-X-C motif chemokine receptor 4; DAT, dopamine active transporter; EGFR, epidermal growth factor

receptor; ENT-1, equilibrative nucleoside transporter-1; FAP, fibroblast activation protein; GLUT, glucose transporter; GRPR, gastrin releasing peptide receptor; IDH, isocitrate dehydrogenase; LAT1, large neutral amino acid transporter; MCT1/4, monocarboxylate transporter-1/4; PM, plasma membrane; PROT, proline transporter; PSMA, prostate-specific membrane antigen; SGLT2, sodium-glucose cotransporter-2; SMCT1/2, sodium monocarboxylate cotransporter-1/2; SSTR1-5, somatostatin receptor-1 to -5; TSPO, translocator protein; WHO, World Health Organization.

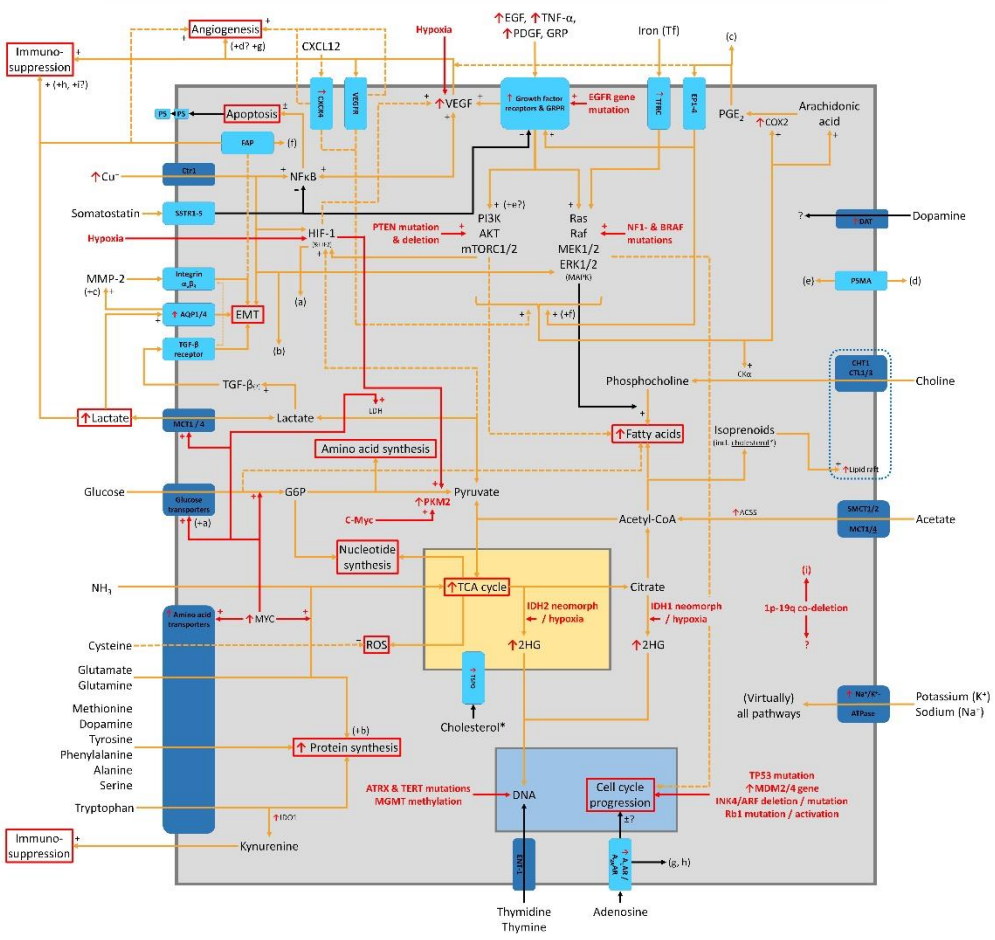

Figure 1 Simplified illustration of key metabolic and regulatory pathways that can be impaired, inhibited or upregulated in tumor cells, including the associated PET agents. The grey box represents the cytoplasm, while the yellow and blue boxes represent mitochondria and nucleus, respectively. Main results of the different pathways are highlighted by red boxes (e.g., increased protein synthesis). Red texts indicate oncogenic or tumoral changes influencing the illustrated pathways. Green texts indicate PET agents. Orange lines (both solid and dashed, different for clarity only) represent upregulated pathways, while normal interactions that are nonetheless relevant for the illustration are shown as black (solid or dashed) lines. The lipid raft (dashed box) was randomly placed, merely illustrating its function of clustering proteins and associated signaling pathways. Dark blue and light blue boxes crossing the plasma membrane represent resp. transporters and receptors.

Abbreviations: 2HG, 2-hydroxyglutarate; A_1AR, A_1 adenosine receptor; A_{2A}AR, A_{2A} adenosine receptor; ACSS, acyl coenzyme A synthetase; AKT, protein kinase B; AQP, aquaporin; ARF, ADP ribosylation factor; ATP, adenosine triphosphate; ATRX, alpha thalassemia / mental retardation syndrome X-linked; BRAF, B-Raf proto-oncogene; CHT1, high-affinity choline transporter; CKα, choline kinase alpha; CoA, acyl coenzyme A; COX, cyclooxygenase; CTL, choline transporter-like protein; Ctr1, copper transporter 1; CXCR4, C-X-C motif chemokine receptor 4 and its ligand CXCL12, C-X-C motif chemokine ligand; DAT, dopamine active transporter; DNA, deoxyribonucleic acid; EGF, epidermal growth factor and EGFR, its receptor; EMT, epithelial-mesenchymal transition; ENT, equilibrative nucleoside transporter; EP, prostaglandin E2 receptor; ERK, extracellular signal-regulated kinases; FAP, fibroblast activation protein; G6P, glucose-6-phosphate; GRP, gastrin releasing peptide and GRPR, its receptor; HIF, hypoxia-inducible factors; IDH, isocitrate dehydrogenase; IDO, indoleamine 2,3-dioxygenase; LDH, lactate dehydrogenase; MAPK, mitogen-activated protein kinase; MCT, monocarboxylate transporter; MDM, E3 ubiquitin-protein ligase; MGMT, O^6-methylguanine-DNA-methyltransferase; MMP, matrix metalloproteinase; mTORC, mechanistic target of rapamycin complex 1; NFκB, nuclear factor kappa-B; NF, neurofibromatosis; PDGF, platelet-derived growth factor; PGE_2, prostaglandin E2; PI3K, phosphatidylinositol 3-kinase; PKM2, pyruvate kinase M2; PS, phosphatidylserine; PSMA, prostate-specific membrane antigen; PTEN, phosphatase and tensin homolog; Rb, retinoblastoma protein; ROS, reactive oxygen species; SMCT, Na^+ monocarboxylate cotransporter; SSTR, somatostatin receptor; TCA, tricarboxylic acid; TERT, telomerase reverse transcriptase; Tf, transferrin; TFRC, transferrin receptor; TGF-β, transforming growth factor beta; TNF-α, tumor necrosis factor alpha; TSPO, translocator protein; VEGF, vascular endothelial growth factor and VEGFR, its receptor.

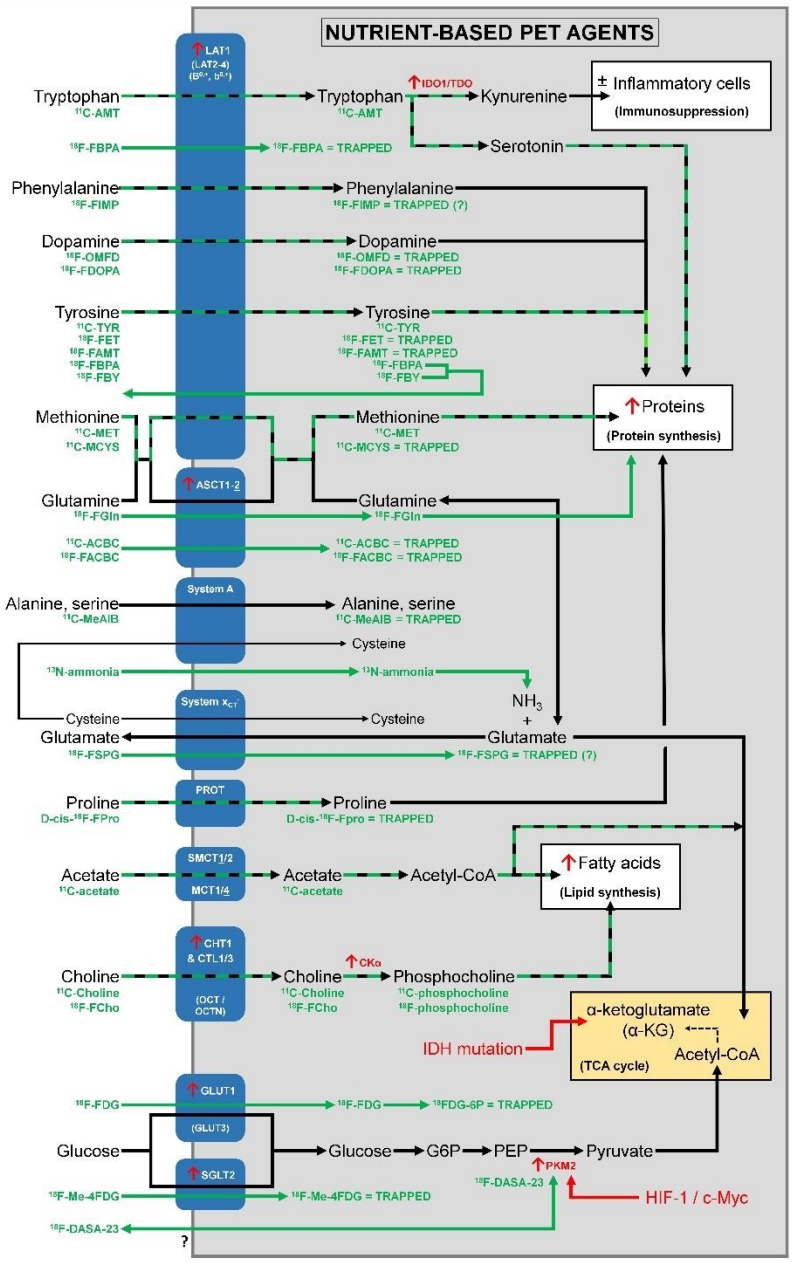

Figure 2 Illustration showing uptake mechanism and assimilation process of nutrient-based PET agents. See also main text. The grey box represents the cytoplasm, while the yellow box represents mitochondria. Green arrows represent metabolic route of specific PET agent, while black arrows represent metabolic route of associated nutrient / building block, and green-black arrows a similar route for PET agent and nutrient / building block. Red text / arrows show brain tumor cell-specific metabolic

alterations. Of note, although ^{11}C-MCYS is a derivative of the amino acid cysteine, it is analogous to ^{11}C-MET and therefore grouped together with ^{11}C-MET in this illustration.

Abbreviations: LAT, large neutral amino acid transporter; IDO, indoleamine 2,3-dioxygenase; ASCT, anti-neutral amino acid transporter; CKα, choline kinase alpha; CoA, acyl coenzyme A; G6P, glucose-6-phosphate; HIF, hypoxia-inducible factors; IDH, isocitrate dehydrogenase; PEP, phosphoenolpyruvate; PKM2, pyruvate kinase M2; PROT, proline transporter; SMCT, Na^+ monocarboxylate cotransporter; MCT, monocarboxylate transporter; CHT1, high-affinity choline transporter; CTL, choline transporter-like protein; OCT / OCTN, organic cation transport proteins; GLUT, glucose transporter; SGLT, sodium-glucose linked transporter; TCA, tricarboxylic acid.

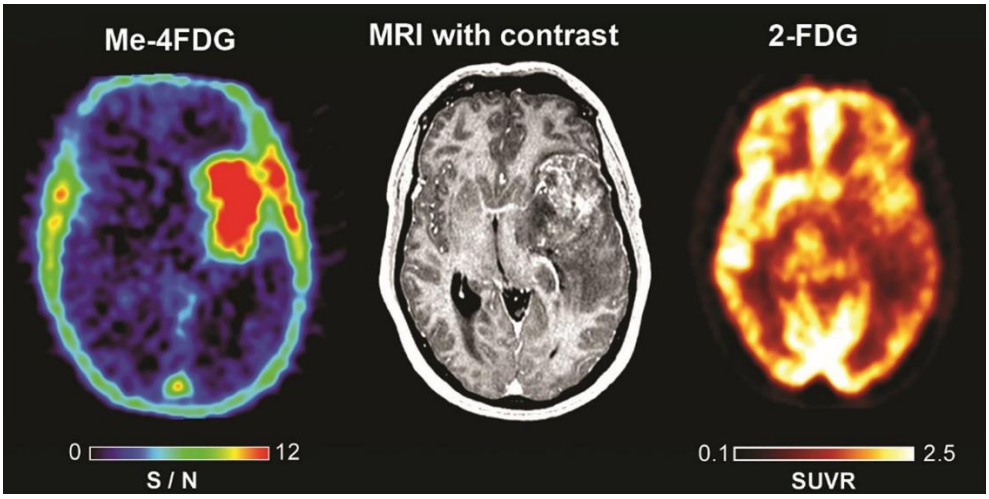

Figure 3 ^{18}F-Me-4FDG PET (left), T_1-weighted post-contrast (middle) and ^{18}F-FDG PET (right) images of a patient with an anaplastic astrocytoma, WHO grade III. The ^{18}F-FDG image shows mixed uptake within some portions of the mass, with highest uptake comparable to normal cortical uptake in the healthy contralateral cortex. The ^{18}F-Me-4FDG image, however, shows uniform tumor uptake without any uptake in the surrounding healthy brain parenchyma, providing significantly higher T/N ratio than the ^{18}F-FDG image. This figure is reproduced – with new figure legend appropriate for current book chapter – from Kepe et al. (2018), Figure 4, under the terms of the Creative Commons Attribution 4.0 International License (http://creativecommons.org/licenses/by/4.0) (48).

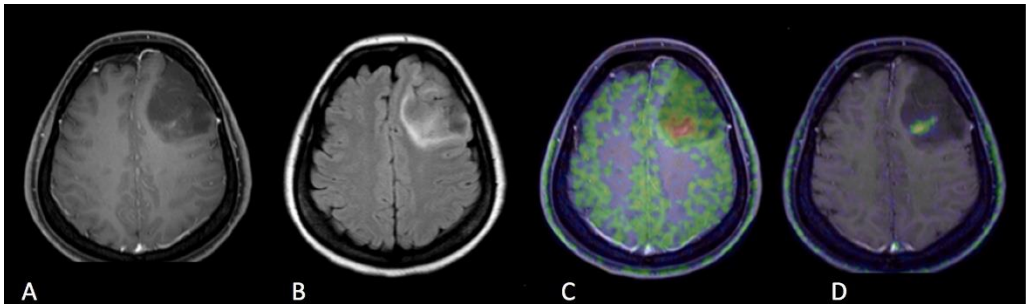

Figure 4 T_1-weighted post-contrast (A), FLAIR (fluid-attenuated inversion recovery; B), ^{11}C-MET PET (C) and ^{18}F-FACBC PET (D) images of a patient with diffuse astrocytoma, WHO grade II, IDH mutated. The conventional MR images show a poorly enhancing lesion with some high signal surrounding the lesion. Although increased PET agent uptake can be seen in a small part of the tumor on both the ^{11}C-MET and ^{18}F-FACBC PET images, this case also illustrates the relatively high uptake of the natural amino acid-based ^{11}C-MET in the healthy brain parenchyma compared to the unnatural amino-acid based ^{18}F-FACBC which can result in decreased T/N ratios. This figure is reproduced – with new figure legend appropriate for current book chapter – from Tsuyuguchi et al. (2017), Figure 1 Case 1, under the terms of the Creative Commons Attribution License (http://creativecommons.org/licenses/by/3.0) (80).

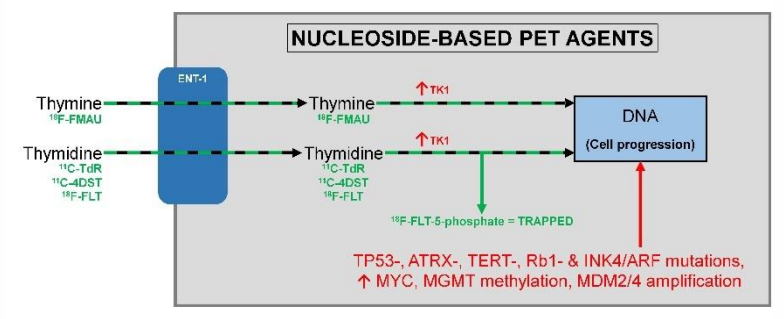

Figure 5 Illustration showing uptake mechanism and assimilation process of the nucleoside-based PET agents. See also main text. The grey box represents the cytoplasm, while the blue box represents the nucleus. Green arrows represent metabolic route of specific PET agent, while black arrows represent metabolic route of associated nutrient / building block, and green-black arrows a similar route for PET agent and nutrient / building block. Red text / arrows show brain tumor cell-specific metabolic alterations.

Abbreviations: ARF, ADP ribosylation factor; ATRX, alpha thalassemia / mental retardation syndrome X-linked; DNA, deoxyribonucleic acid; ENT, equilibrative nucleoside transporter; MGMT, O^6-methylguanine-DNA-methyltransferase; MDM, E3 ubiquitin-protein ligase; Rb, retinoblastoma protein; TERT, telomerase reverse transcriptase; TK, tyrosine kinase.

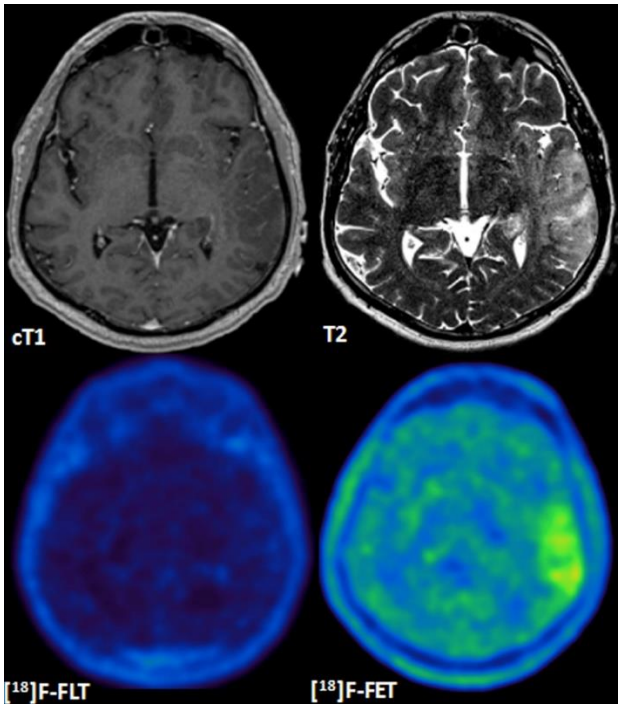

Figure 6 T_1-weighted post-contrast (cT1), T_2-weighted (T2), ^{18}F-FLT PET ([18]F-FLT) and ^{18}F-FET ([18]F-FET) images of a patient with a non-enhancing glioblastoma, WHO grade IV. The lesion is hyperintense on the T_2-weighted image but does not show contrast enhancement. Increased uptake in the T_2-hyperintense region can clearly be seen on the ^{18}F-FET PET image, but there is no uptake visible on the ^{18}F-FLT PET image, illustrating the drawback of PET agents that cannot easily cross the BBB. This figure is reproduced – with new figure legend appropriate for current article – from Nowosielski et al. (2014), Figure 1, under the terms of the Creative Commons Attribution 4.0 International (CC BY) License (http://creativecommons.org/licenses/by/4.0) (107).

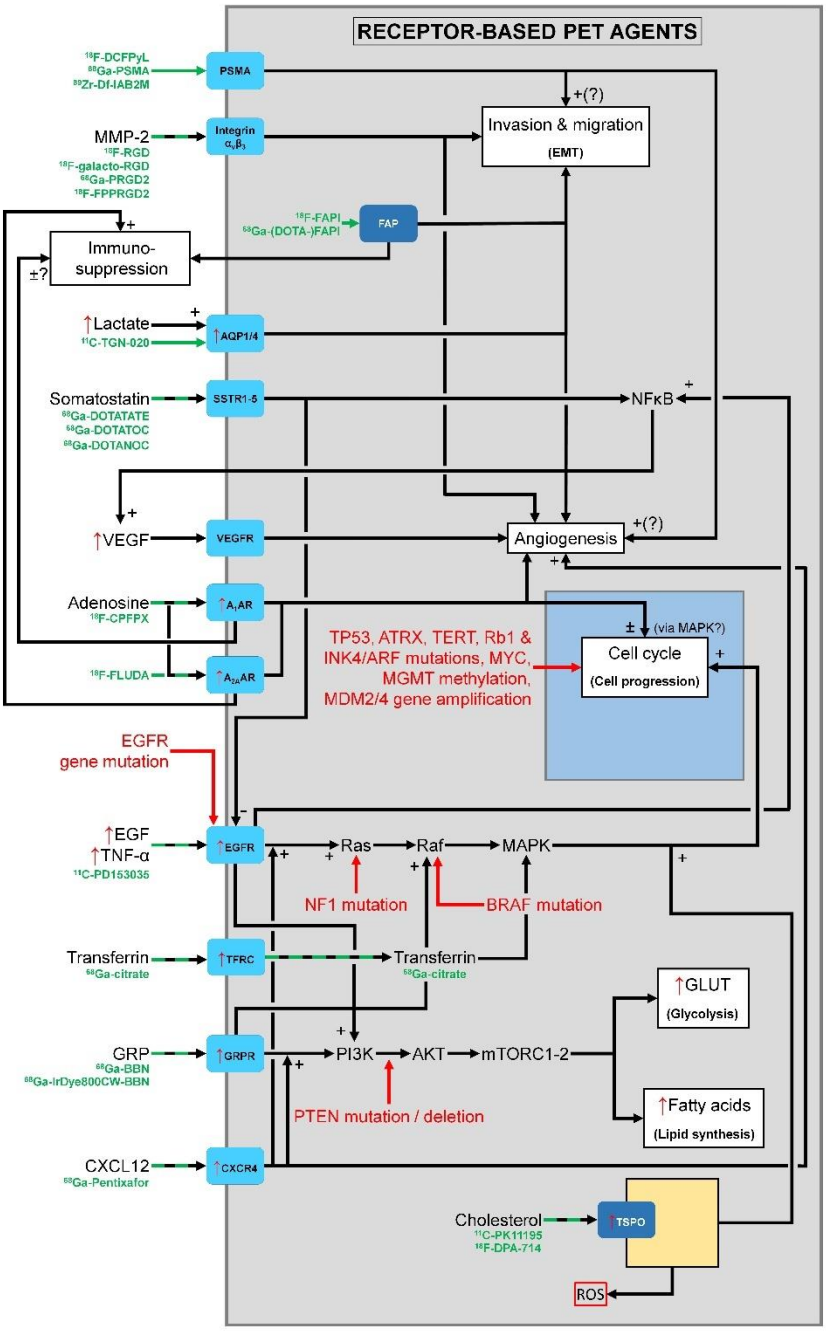

Figure 7 Illustration showing binding mechanism and associated signaling pathways of PET agents that become bound to receptors / transporters. See also main text. The grey box represents the cytoplasm, while the yellow and blue boxes represent mitochondria and nucleus, respectively. Green arrows represent binding of specific PET agent, while black arrows represent signaling pathway of receptor. Red text / arrows show brain tumor cell-specific alterations. Not shown for the sake of clarity: positive effect

of adenosine / adenosine receptor pathway on tumor invasion and migration, as well as on suppressing immune reaction to the tumor.

Abbreviations: A_1AR, adenosine A_1 receptor; A_{2A}AR, adenosine A_{2A} receptor; AKT, protein kinase B; AQP, aquaporin; ARF, ADP ribosylation factor; ATRX, alpha-thalassemia / mental retardation syndrome X; CXCR4, C-X-C motif chemokine receptor 4; CXCL12, C-X-C motif chemokine ligand 12; EGF, epidermal growth factor and EGFR, its receptor; EMT, epithelial-mesenchymal transition; FAP, fibroblast activation protein; GLUT, glucose transporter; GRP, gastrin releasing peptide and GRPR, its receptor; MAPK, mitogen-activated protein kinase; MDM, E3 ubiquitin-protein ligase; MGMT, O^6-methylguanine-DNA-methyltransferase; MMP, matrix metalloproteinase; mTORC, mechanistic target of rapamycin complex 1; NFκB, nuclear factor kappa-B; PI3K, phosphatidylinositol 3-kinase; PSMA, prostate-specific membrane antigen; PTEN, phosphatase and tensin homolog; Rb, retinoblastoma protein; ROS, reactive oxygen species; SSTR, somatostatin receptor; TERT, telomerase reverse transcriptase; TNF-α, tumor necrosis factor alpha; TSPO, translocator protein; VEGF, vascular endothelial growth factor and VEGFR, its receptor.

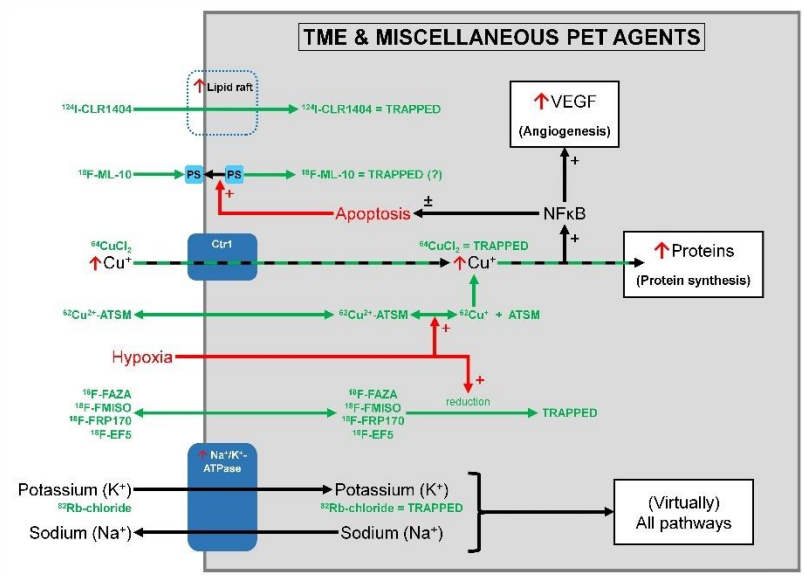

Figure 8 Illustration showing uptake mechanism and assimilation process of nucleoside-based, hypoxia- and miscellaneous (transporter-targeting) PET agents. See also main text. The grey box represents the cytoplasm. Green arrows represent metabolic route of specific PET agent, while black arrows represent metabolic route of associated nutrient / building block, and green-black arrows a similar route for PET agent and nutrient / building block. Red text / arrows show brain tumor cell-specific metabolic alterations.

Abbreviations: Ctr, copper transporter; NFκB, nuclear factor kappa-B; PS, phosphatidylserine; TME, tumor microenvironment; VEGF, vascular endothelial growth factor.

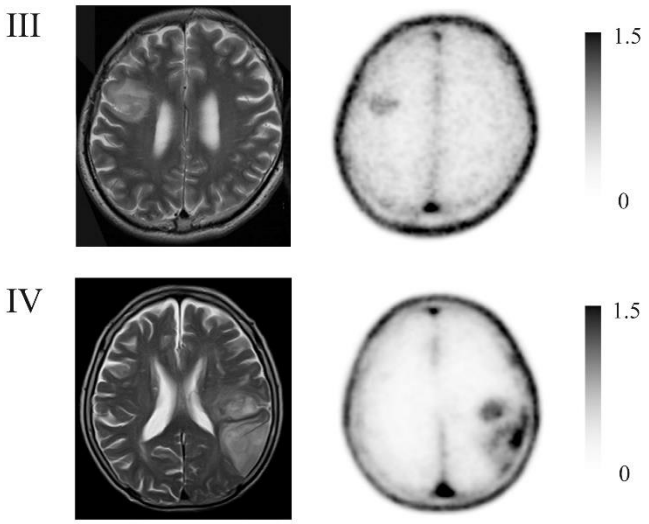

Figure 9 T_2-weighted MR (left) and ^{11}C-TGN-020 PET (right) images of two patients with an astrocytoma WHO grade III (top row) and glioblastoma WHO grade IV (bottom row), respectively. Both tumors show a high T/N ratio; in addition, uptake in the glioblastoma is more intense than in the WHO grade III tumor. This figure is reproduced – with new figure legend (with permission) appropriate for current article – from Suzuki et al. (2018), Figure 1, under the terms of the Creative Commons Attribution-NonCommercial-NoDerivs license (http://creativecommons.org/licenses/bync-nd.4.0/) (159).